

---

## A Multiscale Analysis of Diffusions on Rapidly Varying Surfaces

A. B. Duncan · C. M. Elliott · G. A. Pavliotis ·  
A. M. Stuart

Received: 2 November 2013 / Accepted: 22 January 2015 / Published online: 10 February 2015  
© Springer Science+Business Media New York 2015

**Abstract** Lateral diffusion of molecules on surfaces plays a very important role in various biological processes, including lipid transport across the cell membrane, synaptic transmission, and other phenomena such as exo- and endocytosis, signal transduction, chemotaxis, and cell growth. In many cases, the surfaces can possess spatial inhomogeneities and/or be rapidly changing shape. Using a generalization of the model for a thermally excited Helfrich elastic membrane, we consider the problem of lateral diffusion on quasi-planar surfaces, possessing both spatial and temporal fluctuations. Using results from homogenization theory, we show that, under the assumption of scale separation between the characteristic length and timescales of the membrane fluctuations and the characteristic scale of the diffusing particle, the lateral diffusion process can be well approximated by a Brownian motion on the plane with constant diffusion tensor  $D$  that depends on a highly nonlinear way on the detailed properties of the surface. The effective diffusion tensor will depend on the relative scales of the spatial and temporal fluctuations, and for different scaling regimes, we prove the existence of a macroscopic limit in each case.

---

Communicated by Paul Newton.

---

A. B. Duncan (✉) · G. A. Pavliotis  
Department of Mathematics, Imperial College London, London SW7 2AZ, UK  
e-mail: a.duncan@imperial.ac.uk

G. A. Pavliotis  
e-mail: g.pavliotis@imperial.ac.uk

C. M. Elliott · A. M. Stuart  
Mathematics Institute, Warwick University, Coventry CV4 7AL, UK  
e-mail: C.M.Elliott@warwick.ac.uk

A. M. Stuart  
e-mail: A.M.Stuart@warwick.ac.uk

**Keywords** Homogenization · Laplace–Beltrami · Lateral diffusion · Multiscale analysis · Helfrich elastic membrane · Effective diffusion tensor

**Mathematics Subject Classification** 35Q92 · 60H30 · 35B27

## 1 Introduction

Diffusion processes are ubiquitous in physics, chemistry, and biology (Crank 1979; Berg 1993; Van Kampen 2007). In biology, diffusion plays a fundamental role in many processes occurring at the cellular and subcellular level and is one of the basic mechanisms for intracellular transport (Bressloff and Newby 2013). Diffusion not only occurs within the cell, but can also occur along the cell membrane. This lateral diffusion of molecules along the surface of cells also plays a key role in various cellular processes. The lipid molecules and integral membrane proteins that constitute the cell membrane themselves undergo diffusion along the membrane as a result of thermal agitation (Almeida and Vaz 1995). Lateral diffusion of postsynaptic membrane proteins between synapses is known to play a fundamental part in synaptic transmission (Borgdorff and Choquet 2002; Ashby et al. 2006). Other phenomena in cellular biology in which diffusion over interfaces is involved include vision (Poo and Cone 1974), exo- and endocytosis, signal transduction, chemotaxis, and cell growth (see Sbalzarini et al. 2006; Almeida and Vaz 1995).

Experimental techniques such as single-particle tracking (Saxton and Jacobson 1997), fluorescence recovery after photobleaching (FRAP) (Axelrod et al. 1976), and nuclear magnetic resonance (NMR) (Lindblom and Orädd 1994) have made it possible to accurately measure displacement in a laboratory-fixed plane of molecules diffusing laterally on the surface, and thus to measure the macroscopic diffusion tensor  $D$  of the diffusion process, projected into the plane.

Biological interfaces, however, are not typically flat. Indeed, many membranes will exhibit a nonzero curvature, which is induced by the natural spontaneous curvature of the constituent lipids (Seifert 1997). They may also be rough, i.e., possess spatial microstructure. Moreover, the shape of the membrane is changing in time due to thermal fluctuations and possibly also nonthermal fluctuations induced by active membrane proteins on the surface (Gov 2004).

The geometry of the membrane will cause the macroscopic diffusion tensor  $D$  to be significantly different from the molecular diffusion tensor  $D_0$  of the diffusing protein on the surface itself. The relationship between the molecular diffusion tensor and the macroscopic diffusion tensor has been widely studied for different types of biomembrane. Previous work such as Gustafsson and Halle (1997), Naji and Brown (2007), Halle and Gustafsson (1997), and Sbalzarini et al. (2006) focuses on the problem of lateral diffusion of a particle on a static membrane. Various estimates for  $D$  in terms of the surface fluctuation were derived, most notably the effective medium approximation and area scaling approximation (King 2004; Gustafsson and Halle 1997; Gov 2006; Naji and Brown 2007). Other studies such as Reister and Seifert (2007), Reister-Gottfried et al. (2007), and Reister-Gottfried et al. (2010) have focussed on the problem of diffusion on a thermally excited biomembrane fluctuating in a hydrody-

dynamic medium and derived expressions for the effective diffusion tensor as a function of surface parameters such as bending rigidity, surface tension, and fluid viscosity.

The common factor in these models is the presence of small length and timescales in the resulting evolution equations, which enter due to spatial surface microstructure, or due to rapid temporal fluctuations of the surface or possibly both. The objective of this paper was to investigate the macroscopic behavior of a laterally diffusive process on surfaces possessing microscopic space and timescales using a single, unified mathematical approach. By doing so, we provide rigorous justification for some existing approximations advocated in the literature, clearly explaining the parametric regimes in which they apply and develop a systematic methodology that can be used to study other similar problems. Under the assumption that the slow and fast scales are well separated, it is possible to show that the diffusion process can be approximated by a Brownian motion on the plane, independent of the small scale, but which accounts for the macroscopic effects of the fine spatial structure and rapid fluctuations. We use the classical methods of averaging and homogenization (Bensoussan et al. 1978; Pavliotis and Stuart 2008, particularly for SDEs, as described in the foundational paper Papanicolaou (1977)). Doing so, we derive expressions for the coefficients of the macroscopic process in terms of expectations with respect to a relevant measure that captures the effect of the rapid fluctuations and involves the solution of an auxiliary *cell problem* in the case of homogenization. Although these coefficients will not have a closed form in general, they can be computed numerically, accurately, and efficiently without having to simulate effects at the microscopic level, and they are amenable to analyze in various parameter regimes of interest. In particular, we can obtain bounds on the coefficients in terms of the properties of the surface.

The use of multiscale methods to study lateral diffusion on membranes has been considered before, with varying degrees of rigor. In Gustafsson and Halle (1997), the authors derive the correct macroscopic diffusion tensor for a particle diffusing on a surface with periodic spatial fluctuations basing their result on Jackson and Coriell (1963), Lifson and Jackson (1962), and Festa and d'Agliano (1978), who consider the analogous situation of diffusion in a periodic potential. Under the assumption of symmetry in the spatial fluctuations, the authors then proceed to derive variational bounds for the effective diffusion and provide heuristic arguments for a number of other, tighter approximations. In Naji and Brown (2007), the authors study lateral diffusion on a Helfrich membrane undergoing thermal fluctuations. They identify two limiting regimes: the diffusive limit (homogenization) of a diffusion on a quenched surface and the annealed limit (averaging) of diffusion on a rapidly fluctuating membrane, based on a formal analysis of the Fokker–Planck equation describing the evolution of the system, using an adiabatic elimination of the fast variable as in Risken (1996, Section 8.3). They then use numerical methods to study the dynamics of the intermediate regimes where there is no separation of scales.

However, to our knowledge, there are no studies that adopt a rigorous multiscale approach to solving this problem, nor are we aware of any work that unifies the study of lateral diffusion on surfaces with both rapid spatial and temporal fluctuations in a single framework. Moreover, we are not aware of any study that makes use of multiscale methods to compute the effective diffusion tensor directly rather than via numerical simulation of the multiscale process, with the exception of Abdulle and Schwab (2005)

in which the authors describe an heterogeneous multiscale method (HMM) scheme for computing the solution of an elliptic partial differential equation (PDE) on a static surface possessing fine locally periodic undulations and rigorously prove convergence of the scheme.

In this paper, we consider two simple models for diffusion on a fluctuating surface. The first model describes lateral diffusion on a static surface possessing rapid, periodic fluctuations. Lateral diffusion on quasi-planar periodic surfaces has been previously studied in the literature, mainly in the context of biological interfaces. The first such work we are aware of is [Aizenbud and Gershon \(1985\)](#) where the authors consider the problem of diffusion on a curve possessing rapid periodic fluctuations with the objective of explaining the slowing down of diffusion of *succiny-concanavalin A* receptors on the surfaces of adherent mouse fibroblast. The authors derive the effective diffusion tensor, in this case, given by  $D = \frac{1}{Z^2}$ , where  $Z$  is the average excess surface area of the curved surface relative to its projection on the plane. In [Halle and Gustafsson \(1997\)](#), the authors study the same problem in two dimensions, and by recognizing the problem as diffusion in a periodic potential, they use standard results to obtain the homogenized diffusion tensor  $D$  in terms of the solution of an auxiliary PDE (i.e., the cell problem). Under some implicit symmetry assumptions on the surface, they then derive variational bounds for  $D$ . The authors discuss various nonvariational bounds for the  $D$  and propose two estimates such as the effective medium approximation, given by

$$D_{\text{ema}} = \left\langle \sqrt{|g|}(z) \right\rangle^{-1} \mathbf{I},$$

where  $\sqrt{g}$  is the infinitesimal surface element of the surface and  $\langle \cdot \rangle$  denotes the average with respect to the surface measure and the area scaling approximation given by

$$D_{\text{as}} = \frac{1}{Z} \mathbf{I}. \quad (1)$$

Although both approximations agree at the extremes of weak and strong surface fluctuations, they differ in the intermediate regime. Gustafsson and Halle claim that  $D_{\text{ema}}$  is the better approximation; however, they provide no direct evidence to support this conclusion, which at odds with the numerical experiments demonstrated in [Naji and Brown \(2007\)](#) and with the conclusions of Proposition 3 of this paper. Indeed, we show that in the high-frequency, low-amplitude limit of the surface fluctuations, the diffusion process behaves like a pure diffusion process (i.e., a Brownian motion) on  $\mathbb{R}^d$  with constant macroscopic diffusion coefficient  $D$  and for two-dimensional surfaces, provided  $D$  is isotropic, it is equal to  $D_{\text{as}}$ .

The second model we consider is a generalization of the thermally excited Helfrich elastic membrane model ([Gov 2006](#); [Naji and Brown 2007](#); [Reister and Seifert 2007](#)). The surface is defined by a time-dependent periodic random field undergoing rapid spatial and temporal fluctuations. The macroscopic behavior of laterally diffusing particles on the surface will depend on the relative speed between the spatial and temporal fluctuations. We identify a number of natural distinguished limits for this problem and study the effective properties of the corresponding limit processes and in particular provide a rigorous justification of the effective diffusion estimates derived

in [Naji and Brown \(2007\)](#), [Reister and Seifert \(2007\)](#), [Gustafsson and Halle \(1997\)](#) for lateral diffusion on rapidly fluctuating surfaces.

In [Sect. 2](#) we describe the formulation of lateral diffusion and Brownian motion on a time-dependent, quasi-planar surface. In [Sect. 3](#), we introduce the framework for describing diffusion on a fluctuating surface, applicable to both models. Moreover, we identify four different scaling regimes for the second model. In [Sect. 4](#), we describe a motivating example, namely that of a quasi-planar membrane with Helfrich elastic free energy and show that for small deformations, the dynamics can be described by an Ornstein–Uhlenbeck process for the Fourier modes of the surface ([Granek 1997](#); [Naji and Brown 2007](#)). In [Sect. 5](#), we focus on the first model and using classical periodic homogenization methods, we show that in the macroscopic limit, the projected lateral diffusion process converges to a Brownian motion on the plane with a constant diffusion tensor  $D$ , which can be expressed in terms of the solution to an auxiliary Poisson equation. We study the properties of  $D$  and provide rigorous justification for a number of existing results for similar problems ([Halle and Gustafsson 1997](#); [Naji and Brown 2007](#)).

In [Sects. 6, 7, 8, and 9](#), we study the macroscopic limits of the second model under different scaling regimes. In [Sect. 6](#), we apply the results of [Sect. 5](#) to study the asymptotic behavior of the fluctuating membrane model in the quenched fluctuation regime. In [Sect. 7](#), we consider the problem of lateral diffusion on a surface possessing only rapid temporal fluctuations, a regime which has been well studied for the particular model of a thermally excited Helfrich elastic membrane. Using formal multiscale expansions, we derive the limiting behavior of this model, e.g., [Reister and Seifert \(2007\)](#), [Naji and Brown \(2007\)](#). For the particular case of the Helfrich elastic membrane, we recover the estimates for the effective diffusion tensor given in [Naji and Brown \(2007\)](#), [Halle and Gustafsson \(1997\)](#), [Reister-Gottfried et al. \(2007\)](#). In [Sect. 8](#), we consider diffusion on a surface possessing both spatial and temporal fluctuations with comparable length/timescales. We derive expressions for the limiting equation and study the properties of the effective drift and diffusion tensor. Finally, in [Sect. 9](#), we study the asymptotic behavior of diffusion on a rapidly fluctuating surface possessing both spatial and temporal fluctuations, but where the temporal fluctuations occur at a faster scale than the spatial fluctuations.

In [Sect. 10](#), we consider the particular case of diffusion on a two-dimensional fluctuating Helfrich membrane and exhaustively study the particular limits of this problem. Conclusions regarding the unifying nature and novelty of the multiscale approach to this problem, as well as further avenues of research, are summarized in [Sect. 11](#). Formal justifications of the limit theorems given in this paper are provided in “Appendix.”

## 2 Diffusion on Time-Dependent Surfaces

### 2.1 Preliminaries

In this section, we describe the formulation of Brownian motion moving on a time-dependent surface embedded in  $\mathbb{R}^{d+1}$ . We are primarily interested in quasi-planar membranes, so we will restrict our attention to surfaces that can be represented in

the *Monge parametrization*, that is, surfaces that can be expressed as the graph of a sufficiently smooth function  $H : \mathbb{R}^d \times [0, \infty) \rightarrow \mathbb{R}$ . Such a surface  $S(t)$  can then be parametrized over  $\mathbb{R}^d$  by  $J : \mathbb{R}^d \times [0, \infty) \rightarrow \mathbb{R}^{d+1}$  given by

$$J(x, t) = (x, H(x, t)).$$

The function  $H$  is known as the *Monge gauge*. In local coordinates  $x \in \mathbb{R}^d$ , the metric tensor of  $S(t)$  induced from  $\mathbb{R}^{d+1}$  can be written as

$$G(x, t) = I + \nabla H(x, t) \otimes \nabla H(x, t) \tag{2}$$

and the infinitesimal surface area element is given by  $\sqrt{|G|}(x, t)$ , where

$$|G|(x, t) := \det(G(x, t)) = 1 + |\nabla H(x, t)|^2. \tag{3}$$

It is clear that for any unit vector  $e \in \mathbb{R}^d$ ,

$$1 \leq e \cdot G(x, t)e \leq |G|(x, t), \quad \text{for all } x \in \mathbb{R}^d,$$

so that  $G^{-1}$  is positive definite (though not necessarily uniformly so, since  $|G|(x, t)$  can be arbitrarily large). Throughout this paper, we denote by  $\sqrt{G^{-1}(x, t)}$  or  $G^{-\frac{1}{2}}(x, t)$  the unique positive square root of  $G^{-1}(x, t)$ , such that

$$\left(G^{-\frac{1}{2}}(x, t)\right)^\top \left(G^{-\frac{1}{2}}(x, t)\right) = G^{-1}(x, t), \quad x \in \mathbb{R}^d, t \geq 0.$$

Given  $F : \mathbb{R}^{d+1} \rightarrow \mathbb{R}$  smooth in a neighborhood of  $S(t)$ , the tangential gradient of  $F$  is given in local coordinates by

$$\nabla_{S(t)} F(J(x, t)) = \mathcal{P}(x, t) \nabla F(J(x, t)) = \nabla J(x, t)^\top G^{-1}(x, t) \nabla (F \circ J)(x, t).$$

Here,  $\mathcal{P}(x, t)$  projects vectors in  $\mathbb{R}^{d+1}$  onto the tangential space of  $S(t)$  at local coordinate  $x$ , that is,

$$\mathcal{P}(x, t) = I - \nu(x, t) \otimes \nu(x, t),$$

where  $\nu(x, t)$  is the surface unit normal of  $S(t)$ . The tangential divergence  $\nabla_{S(t)} \cdot$  is then obtained from the tangential gradient by contraction. The generalization of the Laplace operator to curved surfaces is the Laplace–Beltrami operator  $\Delta_{S(t)}$ , which is given by

$$\Delta_{S(t)} F = \nabla_{S(t)} \cdot \nabla_{S(t)} F.$$

One can show (Deckelnick et al. 2005; Dziuk and Elliott 2013) that in local coordinates,  $\Delta_{S(t)}$  acts on functions  $F \in C^2(\mathbb{R}^{d+1})$  as follows:

$$\Delta_{S(t)} F(J(x, t)) = \frac{1}{\sqrt{|G|(x, t)}} \nabla \cdot (\sqrt{|G|(x, t)} G^{-1}(x, t) \nabla (F \circ J)(x, t)),$$

for  $x \in \mathbb{R}^d$ . We thus define the operator  $\mathcal{L}_t$  acting on functions  $f \in C^2(\mathbb{R}^d)$  to be the local coordinate representation of the Laplace–Beltrami operator

$$\mathcal{L}_t f(x, t) = \frac{1}{\sqrt{|G|(x, t)}} \nabla \cdot (\sqrt{|G|(x, t)} G^{-1}(x, t) \nabla f(x, t)), \quad \text{for } x \in \mathbb{R}^d. \quad (4)$$

It is clear that  $\Delta_{S(t)} F(J(x, t)) = \mathcal{L}_t (F \circ J)(x, t)$ , for all  $x \in \mathbb{R}^d, t \geq 0$  and for all  $F \in C^2(\mathbb{R}^{d+1})$ . Notice that for a flat surface, for which  $H \equiv 0$ , the operator reduces to the standard Laplace operator on  $\mathbb{R}^d$ .

### 2.2 Brownian Motion on an Evolving Surface

While the properties of Brownian motion on static surfaces have been widely studied in the applied literature (Van Den Berg and Lewis 1985; Sbalzarini et al. 2006; Almeida and Vaz 1995; Naji and Brown 2007, Brownian motion on time-dependent surfaces has been given less consideration. In Naji and Brown (2007), the authors formally derive the overdamped Langevin equation for diffusion on a surface in the Monge gauge as the limit of a random walk constrained to the surface. In Coulibaly-Pasquier (2011), the author provides a rigorous definition of Brownian motion on a manifold with a time-dependent metric. As we are working entirely in the Monge gauge, we provide the following natural definition of Brownian motion on a fluctuating Monge gauge surface, which is equivalent to that given in Coulibaly-Pasquier (2011) in the graph representation.

**Definition 1** Let  $(\Omega, \mathcal{F}, \mathbb{P})$  be a complete probability space endowed with a right-continuous filtration  $(\mathcal{F}_t)_{t \geq 0}$ . Let  $S(t)$  be a time-dependent surface, with corresponding Monge gauge  $H(x, t)$ , where  $H(\cdot, t) \in C^2(\mathbb{R}^d)$ , for all  $t \geq 0$ . Then, an  $\mathbb{R}^d$ -valued process  $X_x(t)$  defined on  $\Omega \times [0, T)$  is called a Brownian motion on  $S(t)$  started at  $X_x(0) = x \in \mathbb{R}^d$ , if  $X(t)$  is almost surely continuous, adapted with respect to  $\mathcal{F}_t$ , and if for every smooth function  $f : \mathbb{R}^d \rightarrow \mathbb{R}$ ,

$$f(X_x(t)) - f(x) - \int_0^t \mathcal{L}_s f(X_x(s)) \, ds,$$

is a local martingale Karatzas and Shreve (1991, Definition 5.5), where  $\mathcal{L}_s$  is the Laplace–Beltrami operator (4) in local coordinates on  $\mathbb{R}^d$ .

*Remark 1* We note that in the case where  $H \equiv 0$ , Definition 1 reduces to standard Brownian motion on  $\mathbb{R}^d$ .

Let  $S(t)$  be a time-dependent surface with Monge gauge  $H(x, t)$  such that for  $t \in [0, \infty)$ ,  $H(\cdot, t) \in C^2(\mathbb{R}^d)$ . It is possible to obtain a standard Itô SDE that describes Brownian motion on  $S(t)$ . To this end, define  $X_x(t)$  to be the solution of the following Itô SDE

$$\begin{aligned} dX_x(t) &= F(X_x(t), t) \, dt + \sqrt{2\Sigma(X_x(t), t)} \, dB(t), \\ X_x(0) &= x, \end{aligned} \quad (5)$$

where

$$F(x, t) = \frac{1}{\sqrt{|G(x, t)|}} \nabla \cdot \left( \sqrt{|G(x, t)|} G^{-1}(x, t) \right),$$

$$\Sigma(x, t) = G^{-1}(x, t),$$

and  $B(\cdot)$  is a standard  $\mathbb{R}^d$ -valued Brownian motion. By Itô's formula (Theorem 3.3, Karatzas and Shreve 1991), for smooth  $f : \mathbb{R}^d \rightarrow \mathbb{R}$ :

$$\begin{aligned} f(X_x(t)) - f(x) &= \int_0^t \frac{1}{\sqrt{|G|(X_x(s), s)}} \nabla \cdot \left( \sqrt{|G|(X_x(s), s)} \right) \cdot \nabla_x f(X_x(s)) \, ds \\ &\quad + \int_0^t G^{-1}(X_x(s), s) : \nabla_x \nabla_x f(X_x(s)) \, ds \\ &\quad + \int_0^t \sqrt{G^{-1}(X_x(s), s)} \nabla_x f(X_x(s)) \, dB(s) \\ &= \int_0^t \mathcal{L}_s f(X_x(s)) \, ds + M(t), \end{aligned}$$

where  $M(t)$  is a local martingale. It follows that  $X_x(t)$  satisfies the conditions of Definition 1 to be a Brownian motion on the evolving Monge gauge surface  $S(t)$ .

*Remark 2* Note that when the surface is static, then  $X_x(t)$  is equivalent to the local coordinate description of Brownian motion on an  $d$ -dimensional manifold given by Hsu (2002, Equation 3.3.11), up to a scaling of the infinitesimal generator by 2 which we adopt for convenience.

Independently, we may derive from first principles the evolution equation for the probability density  $\rho(z, t)$  of a particle undergoing Brownian motion on a time-dependent surface given in the Monge gauge. The equation corresponds to the Fokker–Planck equation for the SDE (5). Consider a particle undergoing Brownian motion moving on the time-dependent surface  $S(t)$ , and suppose that the process possesses a density  $\rho(t, z)$  with respect to the Lebesgue measure on  $S(t)$ . Let  $\Theta$  be an arbitrary bounded region in  $\mathbb{R}^d$  with smooth boundary, and let  $\mathcal{M}(t)$  be the corresponding region on the fluctuating surface, that is,

$$\mathcal{M}(t) = J(\Theta, t).$$

The density  $\rho(z, t)$  is conserved on the surface  $S(t)$  for all  $t$  such that

$$\int_{S(t)} \rho(z, t) \, dz = 1, \quad \text{for } t \geq 0.$$

Moreover, we assume that  $\rho(z, t)$  flows from one region of  $S(t)$  to another with local Fickian flux  $-\nabla_{S(t)} \rho(z, t)$  where  $\nabla_{S(t)}$ . It follows that  $\rho(z, t)$  satisfies the following equation

$$\frac{\partial}{\partial t} \int_{\mathcal{M}(t)} \rho(z, t) \, dz = - \int_{\partial \mathcal{M}(t)} \nabla_{S(t)} \rho(z, t) \cdot n(z, t) \, dz = \int_{\mathcal{M}(t)} \Delta_{S(t)} \rho(z, t) \, dz,$$

where  $n(z, t)$  is the conormal vector along the boundary of  $\mathcal{M}(t)$ . See [Deckelnick et al. \(2005\)](#) for details. Changing variables from  $z \in S(t)$  to local coordinates  $x \in \mathbb{R}^d$  induces a change in measure  $dz = \sqrt{|G|}(x, t)dx$  where  $|G|$  is given by (3). We can thus rewrite the above equation in local coordinates as

$$\begin{aligned} \frac{\partial}{\partial t} \int_{\Theta} \rho(J(x, t), t) \sqrt{|G|}(x, t) \, dx \\ = \int_{\Theta} \nabla_x \cdot \left( \sqrt{|G|}(x, t) G^{-1}(x, t) \nabla \rho(J(x, t), t) \right) \, dx. \end{aligned}$$

As we are only interested in the diffusion process projected onto the plane, we weight the density  $\rho$  with the surface area element  $\sqrt{|G|}(x, t)$  to compensate for the local changes in area of the surface. To this end, define the density  $q : \mathbb{R}^d \times [0, \infty) \rightarrow \mathbb{R}$  with respect to the Lebesgue measure on  $\mathbb{R}^d$  by

$$q(x, t) := \rho(J(x, t), t) \sqrt{|G|}(x, t).$$

It is straightforward to check that  $\int_{\mathbb{R}^d} q(x, t) \, dx = 1$  for all time  $t$ . Substituting  $q(x, t)$  in the previous equation, and noting that  $\Theta$  is arbitrary, we obtain the following PDE for  $q$  on  $\mathbb{R}^d$

$$\frac{\partial}{\partial t} q(x, t) = \nabla \cdot \left( \sqrt{|G|}(x, t) G^{-1}(x, t) \nabla \left( \frac{q(x, t)}{\sqrt{|G|}(x, t)} \right) \right) = \mathcal{L}_t^* q(x, t), \tag{6}$$

where  $\mathcal{L}_t^*$  is the formal adjoint of  $\mathcal{L}_t$  as defined in (4). We note that the PDE (6) is the Fokker–Planck evolution PDE for a diffusion process with infinitesimal generator given by  $\mathcal{L}_t$  ([Friedman 2006](#), Chapter 6), in particular for the SDE (5). The corresponding backward Kolmogorov equation for the observable  $u(x, t) := \mathbb{E}[u_0(X_x(t))]$  is given by the following PDE:

$$\frac{\partial u(x, t)}{\partial t} = \mathcal{L}_t u(x, t), \quad (x, t) \in \mathbb{R}^d \times (0, \infty), \tag{7a}$$

$$u(x, 0) = u_0(x) \quad x \in \mathbb{R}^d. \tag{7b}$$

### 3 A Simple Model for Membrane Fluctuations

In this section, we introduce a simple model for a fluctuating membrane, which is based on the model for the thermally excited Helfrich membrane derived in [Gov \(2004\)](#), [Naji and Brown \(2007\)](#), and [Reister and Seifert \(2007\)](#). The fluctuating membrane surface is represented in the Monge gauge by a time-dependent random field  $H(x, t)$  over the region  $[0, L]^d$ . We assume that for each  $t \geq 0$ ,  $H(x, t)$  is smooth in  $x$  and  $H(x, t)$  is periodic in  $x$  with period  $L_H$  for each  $t \geq 0$ . Moreover, we shall assume there

is a characteristic timescale  $T_H$  associated with  $H(x, t)$ ; it can be a correlation time when  $H$  is random, or the period when  $H(x, t)$  is periodic in time. Consider a particle diffusing on a realization of the surface  $H(x, t)$  with an isotropic molecular diffusion tensor  $D_0$ . Let  $X(t)$  denote the projected trajectory on  $\mathbb{R}^d$ , and let  $L$  and  $T$  be the macroscopic characteristic length and timescales at which the process  $X(t)$  is being observed. We introduce the notation

$$\begin{aligned} x &= Lx^*, & t &= Tt^*, \\ X(Tt^*) &= LX^*(t^*), \\ H(x, t) &= L_H H^*\left(\frac{x}{L_H}, \frac{t}{T_H}\right), \end{aligned} \tag{8}$$

where  $L_H$  is a scaling constant, so that rescaled function  $H^*$  has period 1 in space. Define the parameters  $\delta$  and  $\tau$  to be

$$\delta = \frac{L_H}{L} \quad \text{and} \quad \tau = \frac{T_H}{T}, \tag{9}$$

which quantify the scale separation between the diffusion process  $X(t)$  and the spatial and temporal fluctuations, respectively. To make explicit the relationship between spatial and temporal fluctuations, we will assume that  $\delta = \varepsilon^\alpha$  and  $\tau = \varepsilon^\beta$  for constants  $\alpha > 0$  and  $\beta \in \mathbb{R}$ . The assumption of rapid fluctuations implies that  $\varepsilon \ll 1$ . Rescaling (5) using (8), dropping the stars, we obtain the following rescaled SDE

$$\begin{aligned} dX^\varepsilon(t) &= \frac{1}{\varepsilon^\alpha} \frac{1}{\sqrt{|G|\left(\frac{X^\varepsilon(t)}{\varepsilon^\alpha}, \frac{t}{\varepsilon^\beta}\right)}} \nabla_y \cdot \left(\sqrt{|G|}G^{-1}\right)\left(\frac{X^\varepsilon(t)}{\varepsilon^\alpha}, \frac{t}{\varepsilon^\beta}\right) dt \\ &\quad + \sqrt{2G^{-1}\left(\frac{X^\varepsilon(t)}{\varepsilon^\alpha}, \frac{t}{\varepsilon^\beta}\right)} dB(t), \end{aligned} \tag{10}$$

where

$$G(y, s) = I + \nabla_y H(y, s) \otimes \nabla_y H(y, s). \tag{11}$$

Let  $\mathbb{K}$  be a finite index set with cardinality  $K = |\mathbb{K}|$ . As a generalization of the Helfrich elastic fluctuating membrane model, we will assume that the random field  $H(x, t)$  can be written as  $H(x, t) = h(x, \eta(t))$ , where

$$h(x, \eta) = \sum_{k \in \mathbb{K}} \eta_k(t) e_k(x),$$

where  $e_k \in C^\infty(\mathbb{T}^d)$ ; these functions can be extended to  $\mathbb{R}^d$  by periodicity. Note that the  $e_k$  need not be orthogonal (although they will be in the examples we consider). We model the stochastic process  $\eta(t)$  as an  $\mathbb{R}^K$ -valued Ornstein–Uhlenbeck (OU) process given by

$$d\eta(t) = -\Gamma \eta(t) dt + \sqrt{2\Gamma\Pi} dW(t), \tag{12}$$

where  $W(\cdot)$  is a standard  $\mathbb{R}^K$ -valued Brownian motion. The drift and diffusion matrices  $\Gamma$  and  $\Pi$  are symmetric, positive definite, and are assumed to commute. Substituting this definition of  $H(x, t)$  into (10), the evolution of the system can be described by the joint process  $(X^\varepsilon(t), \eta^\varepsilon(t))$  satisfies the following Itô SDE

$$dX^\varepsilon(t) = \frac{1}{\varepsilon^\alpha} F\left(\frac{X^\varepsilon(t)}{\varepsilon^\alpha}, \eta^\varepsilon(t)\right) dt + \sqrt{2\Sigma\left(\frac{X^\varepsilon(t)}{\varepsilon^\alpha}, \eta^\varepsilon(t)\right)} dB(t), \tag{13a}$$

$$d\eta^\varepsilon(t) = -\frac{1}{\varepsilon^\beta} \Gamma \eta^\varepsilon(t) dt + \sqrt{\frac{2\Gamma\Pi}{\varepsilon^\beta}} dW(t) \tag{13b}$$

where  $F : \mathbb{T}^d \times \mathbb{R}^K \rightarrow \mathbb{R}^d$  is given by

$$F(x, \eta) := \frac{1}{\sqrt{|g|(x, \eta)}} \nabla \cdot \left(\sqrt{|g|}g^{-1}\right)(x, \eta), \tag{14}$$

$\Sigma : \mathbb{T}^d \times \mathbb{R}^K \rightarrow \mathbb{R}_{\text{sym}}^{2 \times 2}$  is

$$\Sigma(x, \eta) := g^{-1}(x, \eta), \tag{15}$$

and

$$g(x, \eta) := I + \nabla h(x, \eta) \otimes \nabla h(x, \eta). \tag{16}$$

Since  $\Gamma$  and  $\Pi$  commute, it is straightforward to check that the OU process  $\eta^\varepsilon(t)$  is ergodic, with unique invariant measure given by

$$\mu_\eta = \mathcal{N}(0, \Pi), \tag{17}$$

with density

$$\rho_\eta(\eta) \propto \exp\left(-\frac{\eta \cdot \Pi^{-1}\eta}{2}\right), \tag{18}$$

with respect to the Lebesgue measure on  $\mathbb{R}^K$ . Since  $\eta(t)$  converges exponentially fast to its invariant distribution, it is reasonable to assume that  $\eta(t)$  is started in the stationary distribution, i.e.,  $\eta(0) \sim \mu_\eta$ , for the sake of simplicity.

Rather than study the asymptotic behavior of  $X^\varepsilon(t)$  as  $\varepsilon \rightarrow 0$ , it is often more convenient to consider the corresponding backward Kolmogorov equation (7) corresponding to the system of SDEs (13). This PDE describes the time evolution of  $u^\varepsilon : \mathbb{R}^d \times \mathbb{R}^K \times [0, T) \rightarrow \mathbb{R}$  given by

$$u^\varepsilon(x, \eta, t) = \mathbb{E}\left[u(X^\varepsilon(t)) \mid (X^\varepsilon(0), \eta^\varepsilon(0)) = (x, \eta)\right],$$

for a given observable  $u(\cdot)$  as follows:

$$\frac{\partial u^\varepsilon(x, \eta, t)}{\partial t} = \mathcal{L}^\varepsilon u^\varepsilon(x, \eta, t), \quad \text{for } (x, \eta, t) \in \mathbb{R}^d \times \mathbb{R}^K \times (0, T), \tag{19a}$$

$$u^\varepsilon(x, \eta, 0) = v(x, \eta), \quad \text{for } (x, \eta) \in \mathbb{R}^d \times \mathbb{R}^K. \tag{19b}$$

One can then employ homogenization methods for PDEs to identify the homogenized Kolmogorov backward equation in the limit  $\varepsilon \rightarrow 0$ , from which one can read off the homogenized SDE for  $X^0(t)$ . This correspondence between SDE and PDE has been widely employed to study the homogenization and averaging of stochastic processes, see, for example, Pavliotis and Stuart (2008), Bensoussan et al. (1978), Pavliotis et al. (2007).

The infinitesimal generator  $\mathcal{L}^\varepsilon$  can be written as

$$\mathcal{L}^\varepsilon f(x, \eta) = \mathcal{L}_1^\varepsilon f(x, \eta) + \mathcal{L}_2^\varepsilon f(x, \eta).$$

The operator

$$\mathcal{L}_1^\varepsilon f(x) := \frac{1}{\sqrt{|g|(x/\varepsilon^\alpha, \eta)}} \nabla_x \cdot \left( \sqrt{|g|(x/\varepsilon^\alpha, \eta)} g^{-1}(x/\varepsilon^\alpha, \eta) \nabla_x f(x) \right),$$

encodes the effect of the rapid spatial fluctuations, while

$$\mathcal{L}_2^\varepsilon f(\eta) := \frac{1}{\varepsilon^\beta} \left( -\Gamma \eta \cdot \nabla_\eta + \Gamma \Pi : \nabla_\eta \nabla_\eta f \right),$$

describes the rapid temporal fluctuations.

The following proposition establishes the well posedness of Eq. (13) for the joint process  $(X^\varepsilon(t), \eta^\varepsilon(t))$ .

**Proposition 1** *Let  $X_0$  and  $\eta_0$  be random variables, independent of  $B(\cdot)$  and  $W(\cdot)$  such that  $\mathbb{E}[X_0]^2 < \infty$  and  $\mathbb{E}[\eta_0]^2 < \infty$ . Then, the system of SDEs (13) has a unique strong solution  $(X^\varepsilon(t), \eta^\varepsilon(t))$  satisfying  $X(0) = X$  and  $\eta(0) = \eta_0$ . Moreover, the solution  $(X^\varepsilon(t), \eta^\varepsilon(t)) \in C([0, T]; \mathbb{R}^d \times \mathbb{R}^K)$ .  $\square$*

Our objective was to study the behavior of  $X^\varepsilon(t)$  and of solutions to the corresponding backward Kolmogorov equation as  $\varepsilon \rightarrow 0$ . The parameters  $\alpha$  and  $\beta$  quantify the relative speed between the spatial and temporal fluctuations, respectively. Thus, we expect that the limiting behavior will vary for different values of  $\alpha$  and  $\beta$ . In this paper, we will study the asymptotic behavior of the coupled system in the following cases, which are demonstrative of the different possible limiting behaviors of the system.

Case I:  $\alpha = 1$  and  $\beta = -\infty$

In this regime, the temporal fluctuations occur on a timescale slower than the characteristic timescale of the diffusion process, so that the regime captures the macroscopic behavior of a particle diffusing laterally over a stationary realization of the random surface field  $h(x, \eta)$ . This situation has been studied in the case of diffusion on a Helfrich elastic membrane with quenched thermal fluctuations in Naji and Brown (2007).

Case II:  $\alpha = 0$  and  $\beta = 1$

In this regime, the microscopic fluctuations are due to the temporal fluctuations. The motivating example in this regime is that of diffusion on a Helfrich elastic membrane with annealed fluctuations; this problem has been studied in detail Naji and Brown (2007), Gustafsson and Halle (1997), Reister and Seifert (2007).

Case III:  $\alpha = 1$  and  $\beta = 1$

In this regime, we consider lateral diffusion on surfaces possessing both rapid spatial and temporal fluctuations, with the spatial and temporal fluctuations occurring at comparable scales. While this regime has not been studied before, it naturally extends the work covered in [Halle and Gustafsson \(1997\)](#), [Naji and Brown \(2007\)](#), [Reister and Seifert \(2007\)](#) and helps provide a complete picture.

Case IV:  $\alpha = 1$  and  $\beta = 2$

In this regime, we consider surfaces with both rapid spatial and temporal fluctuations but the temporal fluctuations occur at a faster scale compared to the spatial fluctuations. As in Case III, this regime has not been considered previously.

In each of the above cases, we will show that the lateral diffusion process  $X^\varepsilon$  is asymptotically characterized by a limiting diffusion process with constant diffusion tensor and drift term which will be qualitatively different in each case.

Before considering the above four regimes for the fluctuating membrane model, we first consider the problem of lateral diffusion on a static, periodic surface. The diffusion process  $X^\varepsilon(t)$  can be described by an SDE with rapidly varying, periodic coefficients. In Sect. 5, we use standard periodic homogenization techniques to show that the asymptotic behavior is that of a Brownian motion on  $\mathbb{R}^d$  with constant diffusion tensor  $D$ . The resulting analysis serves as a basis for the subsequent models.

In the Case I regime, considered in Sect. 6, each stationary realization of the random field gives rise to a homogenized diffusion tensor. As in [Naji and Brown \(2007\)](#), we consider the average homogenized diffusion coefficient as the effective diffusion tensor in this regime. In the Case II regime considered in Sect. 7, the limiting behavior is determined by the properties of the stationary distribution of the OU process  $\eta(t)$  and deriving the effective diffusion process can be viewed as an averaging problem ([Pavliotis and Stuart 2008](#)).

In the regimes covered by Case III and Case IV, we must consider the interaction between the temporal and spatial fluctuations. In the Case III regime, considered in Sect. 8, the spatial fluctuations homogenize the diffusion process “faster” than the temporal fluctuations, and the result is that the effective diffusion tensor will merely be the effective diffusion tensor from Case I averaged over the invariant measure of the OU process  $\eta(t)$ . This macroscopic limit was considered in [Garnier \(1997\)](#). Deriving the asymptotic behavior in the Case IV regime, considered in Sect. 9, proves more complicated due to the fact that the “fast process” that characterizes the rapid spatial and temporal fluctuations does not possess an explicit invariant measure. Once the geometric ergodicity of the fast process with respect to a unique invariant measure is established, the approach is similar to the classical probabilistic homogenization arguments of [Bensoussan et al. \(1978\)](#). Although a limiting equation is established, the lack of an explicit invariant measure makes it hard to establish bounds on the effective diffusion tensor.

We have not yet addressed the question of the limiting behavior of  $X^\varepsilon(t)$  for other values of  $\alpha$  and  $\beta$  besides those considered in Cases I–IV. The answer to this question is dependent on the properties of the surface  $H(x, t)$ . However, in Sect. 10, for the particular case of diffusion on a thermally fluctuating Helfrich surface, we will show that the limits corresponding to Case I to Case IV are exhaustive, in the sense that these are the only distinguished limits that can arise from this system.

#### 4 Motivating Example: The Helfrich Elasticity Membrane Model

In this section, we describe a particular model of surface fluctuations, namely thermally excited Helfrich elastic membranes. The Canham–Helfrich theory for biological membranes, originally developed by [Canham \(1970\)](#) and [Helfrich \(1973\)](#), is a classical continuum model for studying the macroscopic properties of lipid bilayers. The problem of diffusions on Helfrich elastic surfaces in the context of integral protein diffusion on lipid bilayers was studied in various works, in particular [Naji and Brown \(2007\)](#), [Reister and Seifert \(2007\)](#), [Lin and Brown \(2004\)](#), [King \(2004\)](#). Throughout the paper, we shall revisit this problem as a prototypical example to which the theory can be applied, exhaustively exploring the different scaling limits of this model.

As in all the previous works, we represent the quasi-planar membrane as a two-dimensional time-dependent surface with Monge Gauge  $H$ , periodic over the square  $[0, L]^2$ , where the equilibrium of the fluctuations is governed by the following harmonic approximation to the Helfrich Hamiltonian

$$\mathcal{H}[H] = \frac{1}{2} \int_{[0, L]^2} \left[ \kappa (\Delta H(y))^2 + \sigma (\nabla H(y))^2 \right] dy. \quad (20)$$

Here, the scalars  $\kappa$  and  $\sigma$  denote the bending rigidity and surface tension, respectively. The surface is coupled with a low-Reynolds number hydrodynamic medium. Using an analogous approach as in [Doi and Edwards \(1988\)](#) for polymer dynamics, under the assumption of linear response, the dynamics of the surface fluctuations will be described by the following SPDE

$$\frac{dH(t)}{dt} = RAH(t) + \zeta(t), \quad (21)$$

where  $AH(t)$  is the restoring force for the free energy  $\mathcal{H}$ , that is,

$$AH(t) = -\frac{\delta \mathcal{H}}{\delta H}[H(t)] = -\kappa \Delta^2 H(t) + \sigma \Delta H(t)$$

The operator  $R$  which characterizes the effect of nonlocal interactions of the membrane through the hydrodynamic medium is given by

$$Rf(x) = (\Lambda * f)(x), \quad f \in L^2([0, L]^2)$$

where  $*$  denotes convolution, and  $\Lambda(x)$  is given by the diagonal part of the Oseen tensor, [Kim and Karrila \(1991\)](#):

$$\Lambda(x) = \frac{1}{8\pi\lambda|x|},$$

where  $\lambda$  is the viscosity of the surrounding hydrodynamic medium.

The space–time fluctuations are given by  $\zeta(t)$ , a centered Gaussian random field white in time and with spatial fluctuations having covariance operator  $2k_B T R$ , where

$k_B T$  is the system temperature. From linear response theory, it follows that the dynamics in (21) satisfy the fluctuation–dissipation relation, required to ensure that, formally, the invariant measure is proportional to  $\exp(-\mathcal{H}/(k_B T))$ .

Rescaling the domain to  $\mathbb{T}^2 = [0, 1]^2$ , let  $\{e_k \mid k \in \mathbb{K}_\infty\}$  be the standard Fourier basis for  $L^2(\mathbb{T}^2)$  with periodic boundary conditions, indexed by

$$\mathbb{K}_\infty = \mathbb{Z}^2 \setminus \{(0, 0)\}.$$

It is straightforward to check that the invariant measure of  $H(t)$  is given by the Gaussian measure  $\mathcal{N}(0, \mathcal{C})$  where

$$\mathcal{C} \propto \sum_{k \in \mathbb{K}_\infty} \left( \kappa |2\pi k|^4 + \sigma L^2 |2\pi k|^2 \right)^{-1} e_k(x) \otimes e_k(x).$$

The operator  $\mathcal{C}^{-\frac{1}{2}}$  satisfies Assumptions 2.9 (i)–(iv) of Stuart (2010), so that its spectrum grows commensurately with the spectrum of  $-\Delta$ . It follows from Stuart (2010, Lemma 6.25) that the stationary realizations of the random field will be Hölder continuous with exponent  $\alpha < 1$ , but not for  $\alpha = 1$ . This implies that realizations are not sufficiently regular to allow well-defined tangents at every point on the surface. Indeed,  $H(x, t)$  will be almost surely nowhere differentiable with respect to  $x$  so that it is not possible to consider a laterally diffusive process on a realization of this random field. We must thus introduce an ultraviolet cutoff by setting  $\langle e_k, \mathcal{C} e_k \rangle = 0$  for wavenumbers  $k \notin \mathbb{K}$ , where

$$\mathbb{K} = \{k \in \mathbb{K}_\infty \mid |k| \leq c\},$$

for some fixed constant  $c > 0$  and define  $K = |\mathbb{K}|$ . Looking for solutions  $H(x, t)$  of the form  $H(x, t) = h(x, \eta(t))$ , for  $h : \mathbb{T}^2 \times \mathbb{R}^K$  given by

$$h(x, \eta) = \sum_{k \in \mathbb{K}} \eta_k e_k(x),$$

after substituting in (21), we note that the SPDE diagonalizes to obtain a system of Ornstein–Uhlenbeck processes describing the dynamics of the Fourier modes.

Having described the out-of-equilibrium dynamics of a fluctuating Helfrich surface described by  $h(x, \eta(t))$ , consider the trajectory  $X(t)$  of a particle undergoing lateral diffusion on this surface with scalar molecular diffusion tensor  $D_0$ . After nondimensionalization, we obtain the following system of equations

$$dX^\varepsilon(t) = F(X^\varepsilon(t), \eta^\varepsilon(t)) dt + \sqrt{2\Sigma(X^\varepsilon(t), \eta^\varepsilon(t))} dB(t), \tag{22a}$$

$$d\eta^\varepsilon(t) = -\frac{1}{\varepsilon} \Gamma \eta^\varepsilon(t) dt + \sqrt{\frac{2\Gamma\Pi}{\varepsilon}} dW(t) \tag{22b}$$

where  $\varepsilon = D_0 \lambda L$  and where  $F$  and  $\Sigma$  are given by (14) and (15), respectively. The OU process coefficients are determined by  $\Gamma = \text{diag}(\Gamma_k)$  with

$$\Gamma_k = \frac{\kappa^* |2\pi k|^4 + \sigma^* |2\pi k|^2}{|2\pi k|} \tag{23}$$

and  $\Pi = \text{diag}(\Pi_k)$  with

$$\Pi_k = \frac{1}{\kappa^* |2\pi k|^4 + \sigma^* |2\pi k|^2}, \tag{24}$$

where  $\kappa^*$  and  $\sigma^*$  are the nondimensional constants given by

$$\kappa^* = \frac{\kappa}{k_B T} \quad \text{and} \quad \sigma^* = \frac{\sigma L^2}{k_B T},$$

respectively. The invariant measure of the  $\mathbb{R}^K$ -valued OU process  $\eta(t)$  is then given by

$$\mathcal{N}(0, \Pi) = \prod_{k \in \mathbb{K}} \mu_k,$$

where for each  $k \in \mathbb{K}$ ,  $\mu_k$  is the invariant measure of  $\eta_k$  given by

$$\mu_k = \mathcal{N}(0, \Pi_k). \tag{25}$$

The parameter  $\chi = \varepsilon^{-1}$  had already been considered in [Naji and Brown \(2007\)](#) where it was called the *dynamic coupling parameter* because it controls the scale separation between the diffusion and the surface fluctuations. For the particular case of band-3 protein diffusion on a human red blood cell, the typical values of parameters give  $\varepsilon \approx 0.3$ , which suggests that  $\varepsilon$  is an appropriate small-scale parameter. Of course, the value of  $\varepsilon$  will vary greatly for different scenarios.

The Helfrich model only prescribes the dynamics of the surface fluctuations, i.e., the coupled system of OU processes. However, from the above discussion, we see that nondimensionalizing the Eq. (22) for lateral diffusion on this surface gives rise to a natural scaling, corresponding to  $(\alpha, \beta) = (0, 1)$  in (13). Nonetheless, as an illustration of our theory, we shall consider the behavior of the Helfrich model under different scaling regimes, as it provides an illuminating example. In particular, for the scalings corresponding to Case I–IV, we will consider the effects of the parameters  $\kappa^*$ ,  $\sigma^*$  on the effective diffusion tensor, and in Sect. 6, we will provide an exhaustive study of the scaling limits of this system.

### 5 Case 0: Diffusion on Static, Periodically Varying Surfaces

In this section, we consider the first case described in Sect. 3, namely lateral diffusion on a prescribed static surface with periodic fluctuations about the plane. More specifically, we consider a fixed surface  $S^\varepsilon$  with Monge gauge

$$h^\varepsilon(x) = \varepsilon h\left(\frac{x}{\varepsilon}\right), \tag{26}$$

where  $\varepsilon$  is a small-scale parameter and  $h$  is a sufficiently smooth real-valued function on  $\mathbb{R}^d$  such that  $h$  and its derivatives are periodic with period 1 in every direction. We make no further assumptions on the geometry of  $S^\varepsilon$ , in particular, the Monge gauge  $h(x)$  need not be a realization of any particular distribution. It is straightforward to see that  $S^\varepsilon$  has metric tensor  $g^\varepsilon(x) = g(x/\varepsilon)$ , where

$$g(x) = I + \nabla h(x) \otimes \nabla h(x), \quad x \in \mathbb{T}^d. \tag{27}$$

We note that the size of the undulations  $|\nabla h^\varepsilon(x)|$  remains constant as  $\varepsilon \rightarrow 0$ . For a given surface  $S^\varepsilon$ , define the *excess surface area*  $Z$  to be the average area of the surface per unit projected surface area, which for a periodic surface defined by (26) is given by

$$\begin{aligned} Z &:= \lim_{R \rightarrow \infty} \frac{1}{(2R)^d} \int_{[-R,R]^d} \sqrt{1 + |\nabla h^\varepsilon(y)|^2} \, dy \\ &= \lim_{R \rightarrow \infty} \frac{1}{(2R)^d} \int_{[-R,R]^d} \sqrt{1 + |\nabla h(y/\varepsilon)|^2} \, dy \\ &= \lim_{R \rightarrow \infty} \frac{1}{(2R)^d} \int_{[-R,R]^d} \sqrt{|g|(y)} \, dy \\ &= \int_{\mathbb{T}^d} \sqrt{|g|(y)} \, dy. \end{aligned} \tag{28}$$

In particular, the excess surface area remains constant as  $\varepsilon \rightarrow 0$ , which suggests that the scaling in (26) is justified.

Consider a particle diffusing along the surface  $S^\varepsilon$  and let  $X^\varepsilon(t)$  denote the projection onto the plane. Following the derivation in Sect. 2.2 with  $H(x, t) = h(x)$  and  $G(x, t) = I + \nabla h(x) \otimes \nabla h(x)$ , independent of time, the evolution of  $X^\varepsilon(t)$  is given by the following Itô SDE

$$dX^\varepsilon(t) = \frac{1}{\varepsilon} F(X^\varepsilon(t)/\varepsilon) \, dt + \sqrt{2\Sigma(X^\varepsilon(t)/\varepsilon)} \, dB(t), \tag{29}$$

where

$$F(x) = \frac{1}{\sqrt{|g|(x)}} \nabla \cdot \left( \sqrt{|g|(x)} g^{-1}(x) \right),$$

and

$$\Sigma(x) = g^{-1}(x).$$

As discussed in Sect. 3, rather than directly study the asymptotic behavior of  $X^\varepsilon(t)$ , we can equivalently study the asymptotic behavior of the backward Kolmogorov equation for an observable  $u^\varepsilon(t, x)$  diffusing laterally on a surface  $h^\varepsilon(t)$ , which can be written in local coordinates as

$$\frac{\partial u^\varepsilon(x, t)}{\partial t} = \mathcal{L}^\varepsilon u^\varepsilon(x, t), \quad (x, t) \in \mathbb{R}^d \times (0, T], \quad (30a)$$

$$u^\varepsilon(t, x) = u(x), \quad (x, t) \in \mathbb{R}^d \times \{0\}. \quad (30b)$$

where

$$\mathcal{L}^\varepsilon f(x) = \frac{1}{\sqrt{|g|(x/\varepsilon)}} \nabla_x \cdot \left( \sqrt{|g|(x/\varepsilon)} g^{-1}(x/\varepsilon) \nabla_x f(x) \right), \quad (31)$$

and where  $u \in C_b(\mathbb{R}^d)$ . The process  $X^\varepsilon(t)$  and  $u^\varepsilon(x, t)$  are connected via the backward Kolmogorov equation [Friedman \(2006, Chapter 6\)](#).

Our objective was to study the effective behavior of  $X^\varepsilon(t)$  and  $u^\varepsilon(x, t)$  as  $\varepsilon \rightarrow 0$ . We will show that as  $\varepsilon \rightarrow 0$ , the  $\mathbb{R}^d$ -valued process  $X^\varepsilon(t)$  will converge weakly to a Brownian motion on  $\mathbb{R}^d$  with constant diffusion tensor  $D$  that depends on the surface map  $h(x)$ . Equivalently, we show that  $u^\varepsilon$  converges pointwise to the solution  $u^0$  of the PDE

$$\frac{\partial u^0(x, t)}{\partial t} = D : \nabla_x \nabla_x u^0(x, t), \quad (x, t) \in \mathbb{R}^d \times (0, T], \quad (32a)$$

$$u^0(t, x) = v(x), \quad (x, t) \in \mathbb{R}^d \times \{0\}. \quad (32b)$$

Since (29) (respectively, (30)) is a SDE (respectively, PDE) with periodic coefficients, the problem is amenable to classical periodic homogenization methods, such as those of [Bensoussan et al. \(1978\)](#), [Zhikov et al. \(1994\)](#), [Pavliotis and Stuart \(2008\)](#), and [Papanicolaou \(1977\)](#). In Sect. 5.1, we state the homogenization result for this model. The result will be justified formally by using perturbation expansions of the PDE in (30). The rigorous proof of this result is presented in [Duncan \(2013\)](#).

### 5.1 The Homogenization Result

For convenience, we introduce the fast process  $Y(t) = \frac{X(t)}{\varepsilon} \bmod \mathbb{T}^d$ . We can then express (29) as the following fast–slow system

$$dX^\varepsilon(t) = \frac{1}{\varepsilon} F(Y^\varepsilon(t)) dt + \sqrt{2\Sigma(Y^\varepsilon(t))} dB(t), \quad (33a)$$

$$dY^\varepsilon(t) = \frac{1}{\varepsilon^2} F(Y^\varepsilon(t)) dt + \sqrt{\frac{2}{\varepsilon^2} \Sigma(Y^\varepsilon(t))} dB(t), \quad (33b)$$

where  $X^\varepsilon(t) \in \mathbb{R}^d$ ,  $Y^\varepsilon(t) \in \mathbb{T}^d$  and  $B(t)$  is a standard Brownian motion on  $\mathbb{R}^d$ . The infinitesimal generator of the fast process is the  $L^2(\mathbb{T}^d)$  closure of

$$\mathcal{L}_0 f(y) = \frac{1}{\sqrt{|g|(y)}} \nabla_y \cdot \left( \sqrt{|g|(y)} g^{-1}(y) \nabla_y f(y) \right), \quad f \in C^2(\mathbb{T}^d). \quad (34)$$

It is straightforward to see that  $\mathcal{L}_0$  is a uniformly elliptic operator with nullspace containing only constants, that is,

$$\mathcal{N}[\mathcal{L}_0] = \{\mathbf{1}\},$$

and

$$\mathcal{N}[\mathcal{L}_0^*] = \{\rho(y)\},$$

where  $\rho(y) = \frac{\sqrt{|g(y)|}}{Z}$ , for  $Z = \int_{\mathbb{T}^d} \sqrt{|g(y)|} \, dy$ .

We expect to be able to compute the homogenizing effect of the fast process  $Y^\varepsilon$  on the slow process  $X^\varepsilon$  and thereby obtain an effective equation that accounts for, but removes explicit reference to, the small scale. Given  $v \in C_b^2(\mathbb{R}^2 \times \mathbb{T}^d)$ , the observable

$$v^\varepsilon(x, y) := \mathbb{E} [v(X^\varepsilon(t), Y^\varepsilon(t)) \mid X^\varepsilon(0) = x, Y^\varepsilon(0) = 0]$$

satisfies the backward Kolmogorov equation given by

$$\frac{\partial v^\varepsilon(x, y, t)}{\partial t} = \mathcal{L}^\varepsilon v^\varepsilon(x, y, t), \quad (x, y, t) \in \mathbb{R}^d \times \mathbb{T}^d \times (0, T], \tag{35}$$

where

$$\mathcal{L}^\varepsilon = \mathcal{L}_2 + \frac{1}{\varepsilon} \mathcal{L}_1 + \frac{1}{\varepsilon^2} \mathcal{L}_0 \tag{36}$$

for

$$\mathcal{L}_1 v(x, y) := F(y) \cdot \nabla_x v(x, y) + 2\Sigma(y) : \nabla_x \nabla_y v(x, y), \tag{37}$$

and

$$\mathcal{L}_2 v(x, y) := \Sigma(y) : \nabla_x \nabla_x v(x, y), \tag{38}$$

and where  $\mathcal{L}_0$  is given by (34). Note that the last term in (37) reflects the correlation of the noise between the fast and slow processes. We wish to study the behavior of  $X^\varepsilon$  and  $v^\varepsilon$  in the limit as  $\varepsilon \rightarrow 0$ , homogenizing over the fast variable  $Y^\varepsilon$  to identify a constant coefficient diffusion equation that approximates the slow process. As the corresponding SDE and PDE have periodic coefficients, we can apply results from classical homogenization theory such as [Bensoussan et al. \(1978\)](#), [Zhikov et al. \(1994\)](#) to prove convergence of  $X^\varepsilon$  and  $v^\varepsilon$  to solutions of limiting equations. In this section, we will state the homogenization result for this problem.

The macroscopic effect of the fast-scale fluctuations is characterized by a *corrector*  $\chi \in C^2(\mathbb{T}^d; \mathbb{R}^d)$ , which is the unique, mean-zero solution of the following Poisson problem

$$\mathcal{L}_0 \chi(y) = -F(y), \quad y \in \mathbb{T}^d. \tag{39}$$

which is guaranteed to exist by the Fredholm alternative for elliptic PDEs ([Gilbarg and Trudinger 2001](#)).

The following theorem states the homogenization result for this scaling regime. A formal derivation using perturbation expansions will be given in section ‘‘Case I’’ of Appendix, which can be used as the basis for a rigorous proof. However, a probabilistic approach based on [Pardoux \(1999, Theorem 3.1\)](#) or [Bensoussan et al. \(1978\)](#) is more

succint. In what follows we will adopt the convention that

$$(\nabla_y \chi(y))_{ij} = \frac{\partial \chi_i}{\partial y_j}(y), \quad \text{for } i, j \in 1, \dots, d$$

see Chapter 2 of [Gonzalez and Stuart \(2008\)](#).

**Theorem 1** *The process  $X^\varepsilon$  converges weakly in  $C([0, T]; \mathbb{R}^d)$  to a Brownian motion  $X^0(t)$  with effective diffusion tensor  $D$  given by*

$$D = \frac{1}{Z} \int_{\mathbb{T}^d} (I + \nabla_y \chi(y)) g^{-1}(y) (I + \nabla_y \chi(y))^\top \sqrt{|g|}(y) dy, \quad (40)$$

where  $Z$  is the excess surface area given by (28).

Moreover, if Eq. (30) has initial data  $u$  independent of the fast variable such that  $u \in C_b^2(\mathbb{R}^d)$ , then the solution  $u^\varepsilon$  of (30) converges pointwise to the solution  $u^0$  of (32) uniformly with respect to  $t$  over  $[0, T]$ .  $\square$

*Remark 3* In the second part of Theorem 1, we assume that the initial condition of the backward Kolmogorov equation for this system depends only on the slow variable  $x$ . While this assumption greatly simplifies the analysis, it is not essential. Indeed, if the initial condition  $u$  also depends on the fast variable, then an *initial layer* arises at  $t = 0$ , which can be resolved by introducing auxiliary correction terms to the multiscale expansion which decay exponentially fast in time. Refer to [Khasminskii and Yin \(1996\)](#), [Bourgeat et al. \(2003\)](#) for a similar scenario.

### 5.2 Properties of the Effective Diffusion Tensor

In the one-dimensional case, by integrating (39) directly, one can show ([Pavliotis and Stuart 2008](#)) that the effective diffusion coefficient is given by

$$D = \frac{1}{Z^2},$$

so that the homogenized Eq. (32) becomes

$$\frac{\partial u_0(x, t)}{\partial t} = \frac{1}{Z^2} \Delta u_0(x, t), \quad (x, t) \in \mathbb{R}^1 \times (0, T]. \quad (41)$$

In two dimensions or higher, it is not possible to solve for the corrector  $\chi$  explicitly, and thus,  $D$  has no closed form. However, we can identify certain properties of the effective diffusion tensor. Let

$$H_{per}^1(\mathbb{T}^d) := \left\{ v \in H^1(\mathbb{T}^d) \mid \int_{\mathbb{T}^d} v(y) dy = 0 \right\},$$

and  $S^d = \{e \in \mathbb{R}^{d+1} \mid |e| = 1\}$ . The following proposition illustrates the basic properties of  $D$ , valid in all dimensions.

**Proposition 2** *Let  $e \in S^{d-1}$ , then*

- (i)  $D$  is a symmetric, positive definite matrix.
- (ii)  $D$  can be characterized via the expression

$$e \cdot De = \inf_{v \in H^1_{per}(\mathbb{T}^d)} L[v, e], \tag{42}$$

where

$$L[v, e] := \frac{1}{Z} \int_{\mathbb{T}^d} (e + \nabla v(y)) \cdot g^{-1}(y) (e + \nabla v(y)) \sqrt{|g|(y)} dy$$

and  $\chi^e = \chi \cdot e$  is the unique minimizer of (42).

- (iii) The following Voigt–Reuss bounds (Zhikov et al. 1994, Section 1.6) hold,

$$e \cdot D_*e \leq e \cdot De \leq e \cdot D^*e$$

where

$$e \cdot D_*e = \frac{1}{Z} e \cdot \left( \int_{\mathbb{T}^d} \frac{g(y)}{\sqrt{|g|(y)}} dy \right)^{-1} e, \tag{43}$$

and

$$e \cdot D^*e = \frac{1}{Z} e \cdot \left( \int_{\mathbb{T}^d} g^{-1}(y) \sqrt{|g|(y)} dy \right) e. \tag{44}$$

- (iv) In particular, the rate of diffusion for the homogenized process is always depleted, i.e.,

$$e \cdot De \leq 1.$$

Thus, comparing the effective behavior of  $X^\varepsilon(t)$  with that of a free Brownian motion on  $\mathbb{R}^d$  with the same microscopic diffusion coefficient  $D_0 = I$ , we see that the rapid surface fluctuations always gives rise to a reduction in the rate of diffusion.

*Proof* Property (ii) follows by noting that the Euler–Lagrange equation for the minimizer of (42) is given by the following Poisson problem

$$\mathcal{L}_0 \chi^e(y) = -F(y) \cdot e, \quad y \in \mathbb{T}^d$$

, which has a unique solution  $\chi^e = \chi \cdot e \in H^1_{per}(\mathbb{T}^d)$ , where  $\chi(y)$  is the solution of (39). Moreover,  $e \cdot De = L[\chi^e, e]$ . It follows that for each unit vector  $e \in \mathbb{R}^d$ ,

$$e \cdot De \leq L[0, e] = \frac{1}{Z} e \cdot \left( \int_{\mathbb{T}^2} g^{-1}(y) \sqrt{|g|(y)} dy \right) e =: e \cdot D^*e,$$

proving the second inequality of (iii). To derive the Voigt–Reuss-type lower bound in (iii), we note that for fixed  $e \in S^{d-1}$ ,

$$e \cdot D_* e := \inf_{\substack{\Phi \in L^2(\mathbb{T}^d)^d \\ \int_{\mathbb{T}^d} \Phi(y) \, dy = 0}} \frac{1}{Z} (e + \Phi(y)) \cdot g^{-1}(y) (e + \Phi(y)) \sqrt{|g|(y)} \, dy \leq D.$$

The corresponding Euler–Lagrange equation is given by

$$g^{-1}(y) (e + \Phi(y)) \sqrt{|g|(y)} = C,$$

where  $C$  is a Lagrange multiplier for the constraint  $\int_{\mathbb{T}^d} \Phi(y) \, dy = 0$ , this can be solved explicitly to show that

$$\Phi(y) + e = \frac{g(y)}{\sqrt{|g|(y)}} \left( \int_{\mathbb{T}^d} \frac{g(y)}{\sqrt{|g|(y)}} \right)^{-1} e,$$

so that

$$e \cdot D_* e = \frac{1}{Z} e \cdot \left( \int_{\mathbb{T}^2} \frac{g(y)}{\sqrt{|g|(y)}} \, dy \right)^{-1} e,$$

thus proving (iii). Moreover, the positive definiteness of  $D$  follows immediately from that of  $D_*$ . Using the fact that  $|g^{-1}| \leq 1$ , it follows that

$$e \cdot D e \leq e \cdot D_* e \leq 1,$$

and thus proving (iv). The symmetry of  $D$  follows from the symmetry of the inverse metric tensor, proving (i). □

By using expression (42), it is possible to obtain variational bounds for  $D$  other than  $D^*$  by minimizing over a proper closed subset of  $H^1_{per}(\mathbb{T}^d)$ . By minimizing over larger subsets, it is possible to obtain increasingly tighter bounds (see [Duncan 2013](#), Chapter 4). However, we have not been able to obtain bounds that are consistently tight over different periodic surfaces using this approach.

### 5.3 The Area Scaling Approximation

For surface fluctuations that are genuinely two-dimensional (i.e., not constant along a particular axis), we cannot expect to find an explicit expression for the solution of the cell equation. Nonetheless, for a large class of two-dimensional surfaces, using a *duality transformation* argument, we are able to exploit symmetries that exist exclusively in the two-dimensional case to obtain an explicit expression for the effective diffusion tensor  $D$ , which is known in the literature as the *area scaling approximation*

$$D_{as} = \frac{1}{Z} \mathbf{I}, \tag{45}$$

where  $Z$  is the excess surface area given by (28). Note that, although  $D_{as}$  is known as an approximation in [Gov \(2004\)](#), [Gustafsson and Halle \(1997\)](#), [King \(2004\)](#), and [Naji](#)

and Brown (2007), we shall show that it provides an *exact* formula for the effective diffusion tensor  $D$  provided that  $D$  is isotropic. An immediate corollary of this fact is that if  $D$  is isotropic, it will depend only on the average excess surface area and not on the particular microstructure of the rough surface.

In their simplest forms, duality transformations provide a means of relating the effective diffusion tensor  $\sigma_*$  obtained through homogenizing an elliptic PDE of the form

$$\begin{aligned}
 -\nabla \cdot \left( \sigma \left( \frac{x}{\varepsilon} \right) \nabla v^\varepsilon(x) \right) &= f, & x \in \Omega \in \mathbb{R}^2 \\
 v^\varepsilon(x) &= 0, & x \in \partial\Omega,
 \end{aligned}$$

the effective diffusion tensor  $\sigma'_*$  of a dual problem, where  $\sigma' = Q^\top \sigma Q$  for a  $90^\circ$  rotation  $Q$ . The existence of such a duality depends strongly on the fact that in two dimensions, the  $90^\circ$  rotation of a divergence-free field is curl-free and vice versa. Such transforms were used firstly in conductance problems in Keller (1963) and subsequently by Matheron (1967), Dykhne (1971), Mendelson (1975), Kohler and Papanicolaou (1982).

**Proposition 3** *In two dimensions,  $D$  satisfies the following relationship*

$$\det(D) = \frac{1}{Z^2}. \tag{46}$$

*Consequently, if  $\lambda_1$  and  $\lambda_2$  are the eigenvalues of  $D$  with  $\lambda_1 \leq \lambda_2$ , then*

$$\frac{1}{Z^2} \leq \lambda_1 \leq \frac{1}{Z} \leq \lambda_2 \leq 1. \tag{47}$$

*In particular, if  $D$  is isotropic, then  $D$  can be written explicitly as*

$$D = \frac{1}{Z} \mathbf{I}.$$

*Proof* The above result follows from a straightforward modification of the standard duality transformation. For a proof using variational principles, see Duncan (2013).  $\square$

When  $D$  is not isotropic, Proposition (3) still provides us with useful constraints on the anisotropy of the effective diffusion tensor. We see that if the macroscopic diffusion is unhindered in the direction corresponding to  $\lambda_1$ , then the effective diffusion will be  $\frac{1}{Z^2}$  in the orthogonal direction, corresponding to a diffusion on a one-dimensional surface. In the other extreme, if  $\lambda_1 = \lambda_2$ , then we have an isotropic diffusion tensor and by the above proposition  $\lambda_1 = \lambda_2 = \frac{1}{Z}$ .

### 5.4 A Sufficient Condition for Isotropy

In all of the previous literature regarding lateral diffusion on two-dimensional biological membranes, it is always assumed that the macroscopic diffusion tensor is isotropic,

i.e., a scalar multiple of the identity. While this is a natural assumption, it is clearly not true in general. In this section, we identify a natural sufficient condition to guarantee the isotropy of the effective diffusion tensor. The condition we will assume is as follows:

$$h(x) = h(Qx), \quad x \in \mathbb{R}^2, \tag{48}$$

where  $Q : \mathbb{R}^2 \rightarrow \mathbb{R}^2$  is a  $\frac{\pi}{2}$  rotation about some point  $\mathbf{O} \in \mathbb{R}^2$ . Without the loss of generality, we assume that  $\mathbf{O} = (0, 0)$ .

**Lemma 1** *Let  $Q \in \mathbb{R}^{2 \times 2}$  be any rotation about the origin. If (48) holds, then*

$$g^{-1}(Qx) = Q g^{-1}(x) Q^T \tag{49}$$

and

$$|g|(Qx) = |g|(x), \tag{50}$$

for all  $x \in \mathbb{R}^2$ . □

We now prove that the above condition is a sufficient condition for the effective diffusion tensor to be isotropic. A similar approach can be found in [Zhikov et al. \(1994, Section 1.5\)](#).

**Theorem 2** *If condition (48) holds, then  $D$  is isotropic.*

*Proof* We use a characterization of  $D$  given by (42), namely

$$e \cdot De = \frac{1}{Z} \inf_{v \in H^1_{per}(\mathbb{T}^2)} (e + \nabla v(y)) \cdot g^{-1}(y) (e + \nabla v(y)) \sqrt{|g|(y)} \, dy.$$

Changing variables  $Qz = y$ , using (49) and (50), we obtain

$$\begin{aligned} e \cdot De &= \frac{1}{Z} \inf_{v \in H^1_{per}(\mathbb{T}^2)} \int_{\mathbb{T}^2} (e + \nabla v(Qz)) \cdot Q g^{-1}(z) Q^T (e + \nabla v(Qz)) \sqrt{|g|(z)} \, dz \\ &= \frac{1}{Z} \inf_{v \in H^1_{per}(\mathbb{T}^2)} \int_{\mathbb{T}^2} \left( Q^T e + Q^T \nabla v(Qz) \right) \\ &\quad \cdot g^{-1}(z) \left( Q^T e + Q^T \nabla v(Qz) \right) \sqrt{|g|(z)} \, dz. \end{aligned}$$

Noting that  $Q^T \nabla v(Qz) = \nabla w(z)$ , where  $w(z) = v \circ Q(z)$ , since  $Q$  is a  $\frac{\pi}{2}$  rotation, it is clear that  $w \in H^1_{per}(\mathbb{T}^2)$  if and only if  $v \in H^1_{per}(\mathbb{T}^2)$ . It follows that

$$e \cdot De = e \cdot Q D Q^T e, \tag{51}$$

for all  $e \in S^1$ . Using the fact that  $D$  is symmetric, one can check directly that (51) implies that  $D$  is a scalar times the identity. □

### 5.5 Numerical Method

To compute the effective diffusion tensor for a general two-dimensional surface, rather than adopt the MCMC approach as in Pavliotis et al. (2007) of generating sample paths of  $X^\varepsilon(t)$  using an Euler scheme and estimating  $D$  from the mean square deviation, we instead use a finite element scheme to solve the cell equation and compute  $D$  directly from (40). The latter approach is preferable in this case as, in two dimensions, assembly of the corresponding linear system of equations is still cheap and the resulting matrix problem is relatively well conditioned, so that it can be solved efficiently using a preconditioned conjugate gradient method. On the other hand, a Monte Carlo approach requires long time simulations or many realizations of the SDE to recover  $D$ . Finally, the finite element scheme described in this section can be applied to compute the effective diffusion tensors in the fluctuating membrane model considered in Sections 6, 7, 8, and 9, whereas the corresponding Monte Carlo simulations would involve solving an extremely stiff system of equations over very long time intervals.

The corrector  $\chi$  is approximated numerically with piecewise linear elements to solve the cell problem (39). For the approximation of  $\chi$ , we use a regular triangulation of the domain  $[0, 1]^2$  with mesh width  $\delta_x$ . To impose the periodic boundary conditions of (39), we identify the boundary nodes of the mesh periodically. Thus, for  $\delta_x = \frac{1}{M}$ ,  $M \in \mathbb{N}$ , the resulting finite element scheme has  $M^2$  degrees of freedom.

The stiffness matrix corresponding to the elliptic differential operator  $\mathcal{L}_0$  is assembled using nodal quadrature (Larsson and Thomée 2009) to compute the local contribution of each triangular element to the stiffness matrix. The load vector corresponding to the right-hand side of the cell equation is computed similarly. Thus, the derivatives of the surface map  $\frac{\partial h}{\partial x_1}$  and  $\frac{\partial h}{\partial x_2}$  are evaluated only at the nodes of the mesh. For simple surfaces, the derivatives can be computed directly for each node. The stiffness matrix  $\mathbb{S}$  corresponding to  $\mathcal{L}_0$  is positive semi-definite, with kernel consisting of constant functions.

Once the stiffness matrix and right-hand side have been assembled, the resulting symmetric matrix equation is solved using a preconditioned conjugated gradient method. Given a piecewise linear approximation  $\chi_{\delta_x}^e$  of the solution of the cell equation, we approximate  $Z$  and the effective diffusion tensor  $D$  using linear quadrature. We note that  $D$  can be written as

$$e \cdot De = \frac{1}{Z} \left[ \int_{\mathbb{T}^d} e \cdot g^{-1}(y) e \sqrt{|g|}(y) dy - \langle \chi^e, \chi^e \rangle_V \right],$$

where

$$\langle \chi^e, \chi^e \rangle_V = \int_{\mathbb{T}^d} \nabla \chi^e(y) \cdot g^{-1}(y) \nabla \chi^e(y) \sqrt{|g|}(y) dy$$

is the energy norm of  $\chi^e$ . Thus, using standard a priori error estimates (Brenner and Scott 2008) for the finite element approximation  $D_{\delta_x}$ , one can show a rate of convergence  $\delta_x^2$  of the approximate effective diffusion tensor  $D_{\delta_x}$  to the exact value  $D$ .

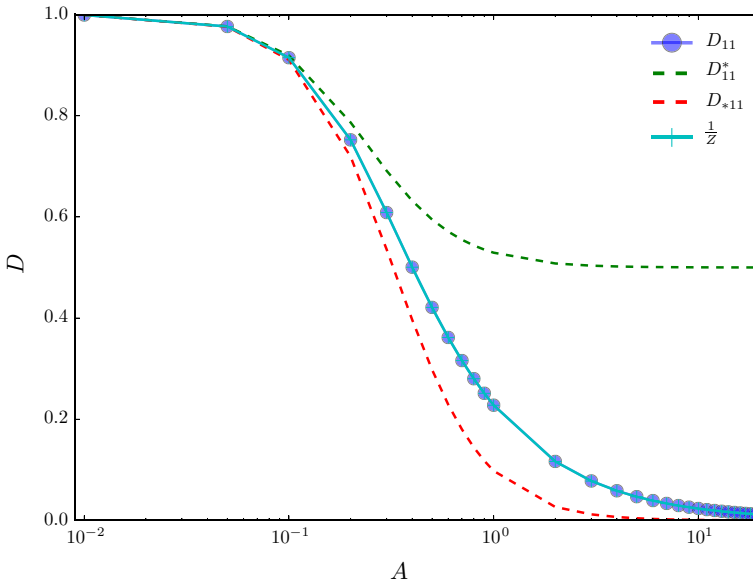


**Fig. 1** Effective diffusion tensor for an “egg-carton” surface with Monge gauge  $h(x) = A \sin(2\pi x_1) \sin(2\pi x_2)$  for varying  $A$ . The dots indicate computed values of  $D$ . The dash-dotted line shows  $D_*$ , and the dashed line shows  $D^*$

### 5.6 Numerical Examples

To illustrate the properties described in the previous sections, we apply the numerical scheme of Sect. 5.5 to numerically compute the effective diffusion tensor for diffusions on various classes of surfaces, along with the bounds  $D^*$ ,  $D_*$  derived in Proposition 2 as well as the area scaling estimate (45).

In Fig. 1, we consider a surface defined by  $h(x) = A \sin(2\pi x_1) \sin(2\pi x_2)$  for varying  $A$ . The isotropy condition holds, so that  $D$  is isotropic and is given by (45). The Voigt–Reuss bounds are sharp in the weak-disorder regime (small  $A$ ) but become increasingly weak as  $A$  increases, with  $D^*$  approaching  $\frac{1}{2}$  in the strong-disorder limit (large  $A$ ) while  $D_*$  converges to 0. As predicted by Proposition 3, the area scaling approximation correctly determines the effective diffusion tensor.

In Figs. 2 and 3, we consider the surface given by

$$h(x) = \sin(2\pi x_1) \sin(6\pi x_2) + A \sin(6\pi x_1) \sin(2\pi x_2).$$

The effective diffusion tensor will not be isotropic except for  $A = 1$ . In Fig. 2, we plot  $D_{11} := e_1 \cdot D e_1$  for varying  $A$ . The Voigt–Reuss bounds  $D^*$  and  $D_*$  are not tight for any  $A$  with  $D^*$  converging to 0.5 as  $A \rightarrow \infty$ . We also see that the area scaling approximation (45) agrees for  $A = 1$ , at which  $D$  is isotropic. In Fig. 3, we plot the maximal and minimal eigenvalues  $D_{\max}$  and  $D_{\min}$  of the effective diffusion tensor. As predicted by (47),  $\frac{1}{2}$  lies between  $D_{\max}$  and  $D_{\min}$ , meeting at  $A = 1$ .

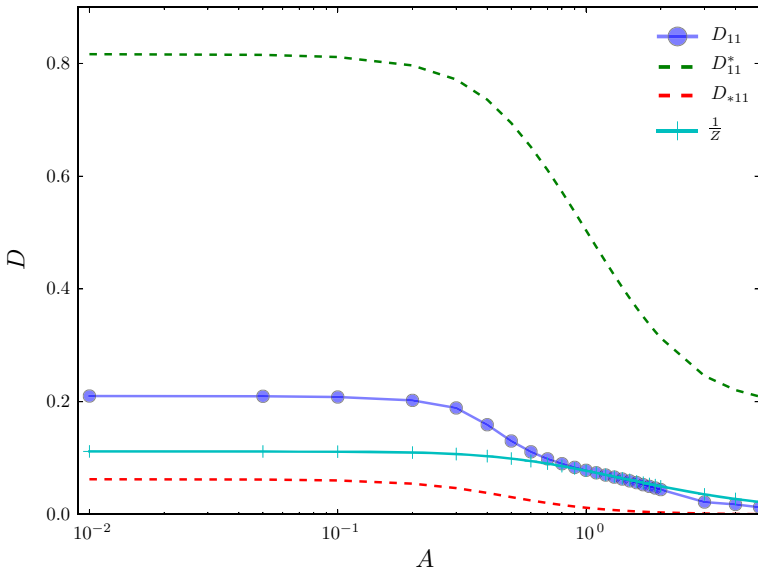


**Fig. 2** Effective diffusion tensor for  $h(x) = \sin(2\pi x_1) \sin(6\pi x_2) + A \sin(6\pi x_1) \sin(2\pi x_2)$ . We plot  $D$  in the  $e_1$  direction

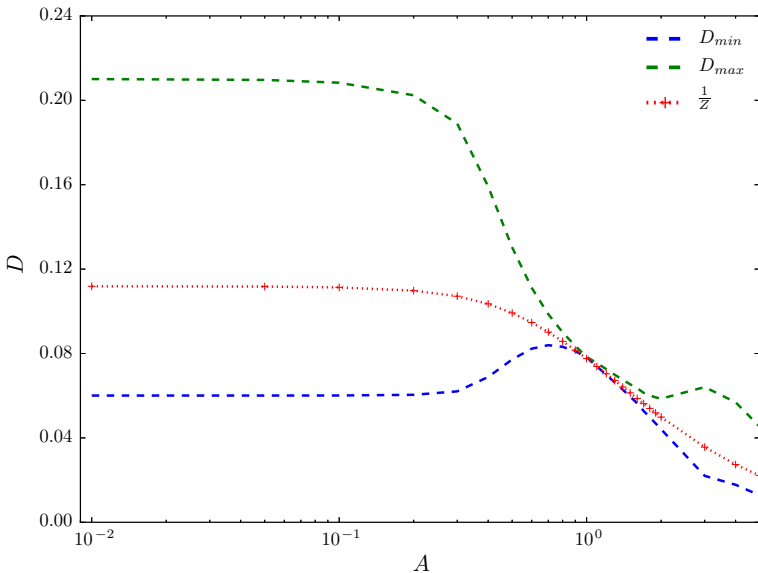


**Fig. 3** Effective diffusion tensor for  $h(x) = \sin(2\pi x_1) \sin(6\pi x_2) + A \sin(6\pi x_1) \sin(2\pi x_2)$ .  $D$  is anisotropic except for  $A = 1$ . The maximal and minimal eigenvalues of  $D$ ,  $D_{\max}$  and  $D_{\min}$ , respectively, are plotted along with the area scaling approximation  $D_{as}$ , illustrating the bound on the eigenvalues given by (47)

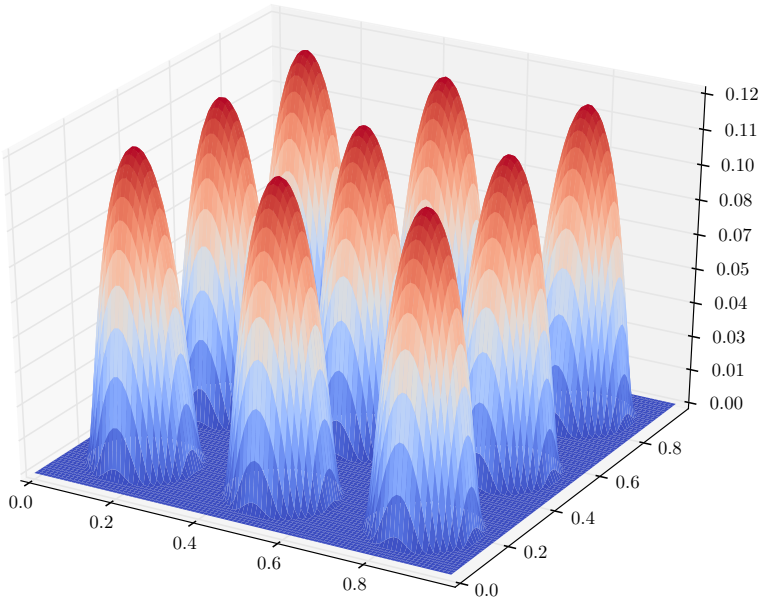


**Fig. 4** A plot of the periodic bump surface with Monge Gauge  $h^\varepsilon(x)$  for  $h(x)$  given by (52) and with  $\varepsilon = \frac{1}{3}$

In Fig. 5, we consider a surface given by a periodic tiling of the standard “bump” function with center  $c = (\frac{1}{2}, \frac{1}{2})$ , radius  $r = 0.45$  and amplitude  $A$ , that is,

$$\begin{aligned}
 h(x) &= A \exp\left(-\frac{1}{1 - \left|\frac{x-c}{r}\right|^2}\right), & |x - c| \leq r \\
 h(x) &= 0 & |x - c| > r.
 \end{aligned}
 \tag{52}$$

A plot of the corresponding multiscale surface for  $\varepsilon = \frac{1}{3}$  is shown in Fig. 4. It is clear that the symmetries of the surface fluctuations will induce an isotropic effective diffusion tensor. We note from Fig. 5 that for  $A < 1.0$ , the effective diffusion is not very sensitive to changes in amplitude, but that it rapidly diminishes as we increase  $A$  beyond 2.

**6 Case I: Diffusion on a Surface with Quenched Fluctuations**

We can apply the results of the previous sections to study the effective behavior of the fluctuating membrane model (29) in the Case I regime where  $(\alpha, \beta) = (1, -\infty)$ , which models a particle diffusing laterally on a static surface obtained by a stationary realization of the process  $\eta(t)$  given in (13). This particular regime had been previously studied in Naji and Brown (2007) for lateral diffusion over a Helfrich elastic membrane with quenched fluctuations. In this section, we will study how the distribution of the surface realization affects the averaged effective diffusion. In Sect. 6.1, we focus on the specific case of a fluctuating Helfrich elastic surface.

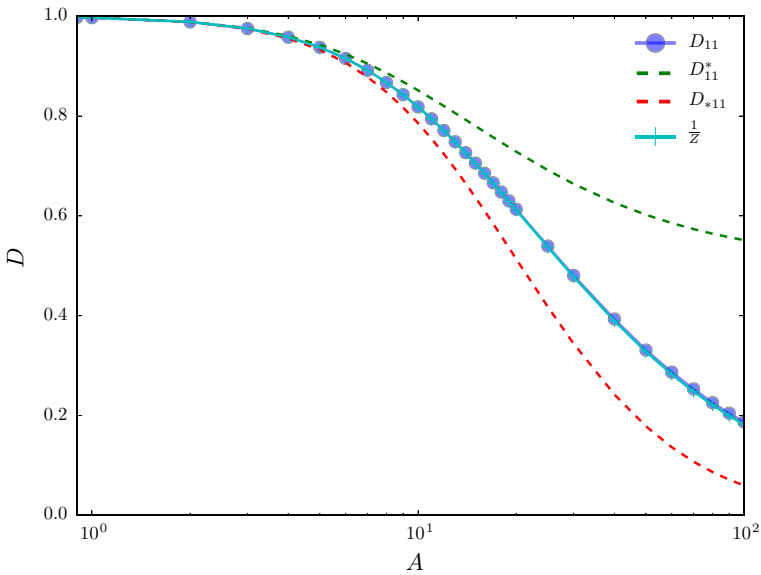


**Fig. 5** Effective diffusion for diffusion on a periodic surface, where each cell is a “bump” with width 0.45 and amplitude  $A$  given by the graph of (52)

By homogenizing the diffusion process over a stationary realization of the surface fluctuations  $\eta$ , we obtain an  $\eta$ -dependent homogenized diffusion tensor. To characterize the effective diffusive behavior of particles on the surface, we define the effective diffusion coefficient  $\bar{D}$  to be the effective diffusion tensor averaged over all stationary surface realizations. To this end, given  $g(y, \eta)$  as in (16), and the stationary density  $\rho_\eta(\eta)$  given by (18), define

$$\rho_y(y, \eta) = \frac{\sqrt{|g(y, \eta)|}}{Z(\eta)}, \tag{53}$$

where  $Z(\eta)$  is the  $\eta$ -dependent excess surface area given by

$$Z(\eta) = \int_{\mathbb{T}^d} \sqrt{|g(y, \eta)|} \, dy.$$

Then, by Theorem 1,  $\bar{D}$  is given by

$$\bar{D} = \int_{\mathbb{R}^K} \int_{\mathbb{T}^d} (I + \nabla_y \chi) g^{-1}(y, \eta) (I + \nabla_y \chi)^\top \rho_y(y, \eta) \rho_\eta(\eta) \, dy \, d\eta, \tag{54}$$

where  $\chi(y, \eta)$  is the unique, mean-zero solution of

$$\nabla \cdot \left( \sqrt{|g(y, \eta)|} g^{-1}(y, \eta) (\nabla \chi(y, \eta) + I) \right) = 0, \quad (y, \eta) \in \mathbb{T}^d \times \mathbb{R}^K. \tag{55}$$

Properties of the effective diffusion tensor such as isotropy depend on the symmetries that exist in the distribution of the random field  $h$ . It is thus more natural to work with a distribution  $\mathbb{P}$  of the periodic random field  $h(y)$ , rather than  $\eta$ . To this end, given the stationary measure  $\mu_\eta$  of the OU, let  $\mathbb{P}$  be the probability measure on  $C(\mathbb{T}^2)$  given by the pushforward of  $\mu_\eta$  under the map  $P : \mathbb{R}^K \rightarrow C(\mathbb{T}^2)$  where

$$P(\zeta) = \sum_{k \in \mathbb{K}} \zeta_k e_k.$$

Given a single realization  $h \in C^\infty(\mathbb{T}^d)$  of  $\mathbb{P}(dh)$ , define  $D(h)$  to be the unique effective diffusion coefficient arising from lateral diffusion on the surface defined by  $h$ , corresponding to (40) in Theorem 1. We can then rewrite  $\bar{D}$  as follows:

$$\bar{D} = \int D(h)\mathbb{P}(dh). \tag{56}$$

The first result we show is an analogue of Proposition 2.

**Proposition 4** *Suppose  $d = 2$  and let  $Q \in \mathbb{R}^{2 \times 2}$  be a rotation by  $\frac{\pi}{2}$ . Define  $\mathcal{Q} : C(\mathbb{T}^2) \rightarrow C(\mathbb{T}^2)$  by*

$$(\mathcal{Q}f) = f(Q^\top \cdot).$$

*Suppose  $\mathbb{P}$  is invariant with respect to  $\mathcal{Q}$ , that is,  $\mathcal{Q}^{-1} \circ \mathbb{P} = \mathbb{P}$ , then  $\bar{D}$  is isotropic.*

*Proof* Let  $h$  be a realization of  $\mathbb{P}$ . Similar to the proof of Proposition 2, we have that

$$\nabla(\mathcal{Q}h)(x) = Q \nabla h(Q^\top x).$$

Denoting by  $g(x, h)$  the metric tensor for the graph of  $h$  evaluated at  $x \in \mathbb{R}^d$ , that is,  $g(x, h) := I + \nabla h(x) \otimes \nabla h(x)$ , then

$$g^{-1}(x, \mathcal{Q}h) = Q g^{-1}(Q^\top x, h) Q^\top$$

and

$$|g|(x, \mathcal{Q}h) = |g|(Q^\top x, h).$$

Let  $D(h)$  be the homogenized diffusion tensor for a particular realization  $h$  of  $\mathbb{P}$ . Then, using a similar argument to that of Proposition 2 gives

$$\begin{aligned} e \cdot D(\mathcal{Q}h)e &= \inf_{v \in H^1_{per}(\mathbb{T}^2)} \int_{\mathbb{T}^2} (\nabla v(x) + e) \cdot Q g^{-1}(Q^\top x, h) Q^\top (\nabla v(x) + e) \sqrt{|g|(Q^\top x, h)} \, dy \\ &= \inf_{w \in H^1_{per}(\mathbb{T}^2)} \int_{\mathbb{T}^2} \left( Q^\top \nabla w(Q^\top x) + Q^\top e \right) \cdot g^{-1}(Q^\top x, h) \end{aligned}$$

$$\begin{aligned} & \times \left( Q^\top \nabla w(Q^\top x) + Q^\top e \right) \sqrt{|g|} (Q^\top x, h) \, dy \\ & = e \cdot Q D(h) Q^\top e. \end{aligned}$$

The result follows immediately from the previous relation since using the invariance of the measure  $\mathbb{P}$  with respect to  $\mathcal{Q}$ :

$$\begin{aligned} \bar{D} &= \int D(h) \mathbb{P}(dh) \\ &= \int D(\mathcal{Q}h) \mathbb{P}(dh) \\ &= \int Q D(h) Q^\top \mathbb{P}(dh) \\ &= Q \bar{D} Q^\top. \end{aligned} \tag{57}$$

Using the fact that  $\bar{D}$  is symmetric, one can check directly that  $\bar{D}$  is isotropic.  $\square$

Although  $\bar{D} = \mathbb{E}_P [D(h)]$  is isotropic, one cannot directly apply the area scaling approximation from Sect. 5.4 to obtain a closed-form expression for  $\bar{D}$ . Two estimates were proposed for  $\bar{D}$  in [Naji and Brown \(2007\)](#), namely the averaged area scaling estimate and effective medium approximation given by

$$\bar{D}_{as} = \mathbb{E}_{\mathbb{P}} \left[ \frac{1}{Z(h)} \right] \mathbf{I} \quad \text{and} \quad \bar{D}_{ema} = \mathbb{E}_{\mathbb{P}} \left[ \frac{Z(h)}{\int |g|(y, h) \, dy} \right] \mathbf{I},$$

respectively. Although both these estimates agree in the limits  $|\nabla h| \ll 1$  and  $|\nabla h| \gg 1$ , they differ in the intermediate regime. Based on numerical experiments, by comparing the values of  $\bar{D}_{ema}$  and  $\bar{D}_{as}$  with diffusion tensors obtained from direct stochastic simulations, the authors of [Naji and Brown \(2007\)](#) concluded that the area scaling estimate  $\bar{D}_{as}$  gives the best agreement with  $\bar{D}$ .

Let  $Q$  be a  $90^\circ$  rotation and define  $\mathcal{Q} : C(\mathbb{T}^d) \rightarrow C(\mathbb{T}^d)$  to be

$$\mathcal{Q}(h) = h(Q \cdot).$$

It is straightforward to see that  $\bar{D} \rightarrow \bar{D}_{as}$  as  $\delta = \mathbb{E}_{\mathbb{P}} |\nabla h|^2 \rightarrow 0$ . Moreover, with the additional assumption that the measure  $\mathbb{P}$  is invariant under  $\mathcal{Q}$ , the following result provides us with a higher-order approximation.

**Theorem 3** *Suppose that*

$$\mathbb{P} \circ \mathcal{Q}^{-1} = \mathbb{P}, \tag{58}$$

*and that  $\delta = \mathbb{E}_{\mathbb{P}} [|\nabla h(y)|^2] \ll 1$ , then for any unit vector  $e \in \mathbb{R}^2$ ,*

$$e \cdot \bar{D} e = e \cdot \bar{D}_{as} e + O(\delta^2). \tag{59}$$

*Proof* We look for solutions of the cell equation

$$\nabla \cdot \left( \sqrt{|g|(y, h)} g^{-1}(y, h) (\nabla \chi^e(y, h) + e) \right) = 0. \tag{60}$$

We look for solutions  $\chi^e$  of (60) satisfying  $\int_{\mathbb{T}^2} \chi^e(y, h) \, dy = 0$  and in the form of a power series in  $\delta$ :

$$\chi^e(y, h) = \chi_0^e(y, h) + \delta \chi_2^e(y, h) + O(\delta^2). \tag{61}$$

Write  $\nabla h(y) = \delta^{\frac{1}{2}} \nabla h_0(y)$ , where  $\mathbb{E} [|\nabla h_0|^2] = 1$ . By Taylor’s theorem, we have that

$$\sqrt{1 + \delta |\nabla h_0(y)|^2} = 1 + \frac{\delta |\nabla h_0(y)|^2}{2} + O(\delta^2). \tag{62}$$

Similarly, we can write

$$\sqrt{|g|(y, h)} g^{-1}(y, h) = \left( 1 - \frac{\delta |\nabla h_0(y)|^2}{2} \right) (I + \delta H(y, h_0)) + O(\delta^2), \tag{63}$$

where  $H(y, h_0) = (\nabla h_0)^\perp \otimes (\nabla h_0)^\perp$ . Substituting (62) and (63) into (60) neglecting terms of order  $\delta^2$  and higher, it follows that

$$\begin{aligned} & -\nabla \cdot \left( \left( 1 - \frac{\delta |\nabla h_0(y)|^2}{2} \right) (I + \delta H(y, h_0)) (\nabla \chi_0^e + \delta \nabla \chi_2^e) \right) \\ & = -\nabla \cdot \left( \left( 1 - \frac{\delta |\nabla h_0(y)|^2}{2} \right) (I + \delta H(y, h_0)) e \right) \end{aligned}$$

Collecting terms of order 0, we get

$$-\Delta \chi_0^e(y, h_0) = \nabla \cdot e = 0, \tag{64}$$

which implies that  $\chi_0^e = 0$  as expected. Similarly, collecting  $O(\delta)$  terms

$$-\Delta \chi_2^e = \nabla \cdot \left( H(y, h_0) e - \frac{|\nabla h_0(y)|^2}{2} e \right). \tag{65}$$

Since the integral of the right-hand side is 0, by the Fredholm alternative, there is a unique solution  $\chi_{e,2}$  with mean zero. The effective diffusion tensor  $D(h)$  can be computed from  $\chi_e$  as follows:

$$\begin{aligned} e \cdot D(h) e &= \frac{1}{Z(h)} \int_{\mathbb{T}^2} e \cdot g^{-1}(y, h) e \sqrt{|g|(y, h)} \, dy \\ &\quad - \frac{1}{Z(h)} \int_{\mathbb{T}^2} \nabla \chi^e(y, h) \cdot g^{-1}(y, h) \nabla \chi^e(y, h) \sqrt{|g|(y, h)} \, dy. \end{aligned} \tag{66}$$

Substituting the above expansions in (66)

$$\begin{aligned}
 e \cdot D(h)e &= \frac{1}{Z(h)} \int_{\mathbb{T}^2} e \cdot \left( 1 - \frac{\delta |\nabla h_0(y)|^2}{2} + O(\delta^2) \right) (I + \delta H(y, h_0)) e \, dy \\
 &\quad - \frac{\delta^2}{Z(h)} \int_{\mathbb{T}^2} \nabla \chi_2^e(y, h_0) \cdot \left( 1 - \frac{\delta |\nabla h_0(y)|^2}{2} + O(\delta^2) \right) \\
 &\quad \times (I + \delta H(y, h_0)) \nabla \phi_2^e(y) \, dy.
 \end{aligned}$$

Collecting terms of equal powers of  $\delta$ :

$$e \cdot D(h)e = \frac{1}{Z(h)} + \frac{\delta}{Z(h)} \int_{\mathbb{T}^2} e \cdot \left( H(y, h_0) - \frac{|\nabla h_0(y)|^2}{2} \right) e \, dy + \delta^2 K(h_0).$$

The  $O(\delta)$  term is given by

$$\int_{\mathbb{T}^2} e \cdot \left( \int \frac{1}{Z(h)} \left[ H(y, h_0) - \frac{|\nabla h_0(y)|^2}{2} I \right] \mathbb{P}(dh) \right) e \, dy. \tag{67}$$

By the assumption of invariance with respect to  $\mathcal{Q}$ , taking expectation with respect to  $\mathbb{P}$ , integrating with respect to  $y$ , and applying Fubini’s theorem, we see that

$$\mathbb{E}_{\mathbb{P}} \int \frac{1}{Z(h)} \left( \frac{\partial h_0}{\partial y_1} \right)^2 \, dy = \mathbb{E}_{\mathbb{P}} \int \frac{1}{Z(h)} \left( \frac{\partial h_0}{\partial y_2} \right)^2 \, dy,$$

and

$$\mathbb{E}_{\mathbb{P}} \int \frac{1}{Z(h)} \frac{\partial h_0}{\partial y_1} \frac{\partial h_0}{\partial y_2} \, dy = 0.$$

It follows that (67) is 0. Therefore, taking expectation on both sides, we have that

$$\bar{D} = \mathbb{E}_{\mathbb{P}} [D(h)] = \mathbb{E}_{\mathbb{P}} \left[ \frac{1}{Z(h)} \right] + \delta^2 \mathbb{E}_{\mathbb{P}} [K(h)].$$

The leading order term of  $K(h)$  is given by

$$K(h) = -\frac{1}{Z(h)} \int_{\mathbb{T}^2} \frac{|\nabla h_0(y)|^2 e \cdot H(y, h_0) e}{2} - \frac{3 |\nabla h_0(y)|^4}{8} + |\nabla \chi_2^e(y, h_0)|^2 \, dy.$$

The fact that  $\mathbb{E}_{\mathbb{P}}[K(h)]$  is bounded follows from the fact that  $\mathbb{P}$  is Gaussian, so  $|\nabla h_0|$  has all moments finite, along with standard  $L^2(\mathbb{T}^2)$  bounds on  $|\nabla \chi_2^e|$ , which follow from (65). □

It follows by Taylor expanding  $\overline{D}_{as}$  that

$$\overline{D} = 1 - \frac{1}{2}\delta + O(\delta^2), \tag{68}$$

for  $\delta = \mathbb{E}_{\mathbb{P}} |\nabla h(y)|^2$ , which gives a first-order approximation for  $\overline{D}$  in the weak-disorder limit (i.e., where  $|\nabla h|$  is small).

Note that the results of this section do not depend explicitly on the fact that  $\mathbb{P}$  is Gaussian, beyond  $\nabla h$  having finite first and second moments. Indeed, the above can be applied to more general distributions.

### 6.1 Diffusion on a Helfrich Surface in the $(\alpha, \beta) = (1, -\infty)$ Regime

We can apply the results of the previous section to study the macroscopic behavior of particles diffusing on a two-dimensional quenched Helfrich elastic membrane. To this end, as in Sect. 4, we set  $\mathbb{K} = \{k \in \mathbb{Z}^2 \setminus \{(0, 0)\} \mid |k| \leq c\}$ , and set the coefficients of  $\eta^\varepsilon(t)$  to be  $\Gamma = \text{diag}(\Gamma_k)_{k \in \mathbb{K}}$  and  $\Pi = \text{diag}(\Pi_k)_{k \in \mathbb{K}}$ , where  $\Gamma_k$  and  $\Pi_k$  are given by (23) and (24), respectively. The spatial variation is then determined by  $\{e_k\}_{k \in \mathbb{K}}$  where  $e_k(x) = e^{2\pi i x}$ .

Since  $\Gamma_k$  and  $\Pi_k$  depend only on  $|k|$ , the conditions for Proposition 4 and Theorem 3 hold trivially. Therefore, the average effective diffusion tensor is isotropic, although individual realizations of  $D(h)$  will not be isotropic in general. This anisotropy will decrease as the magnitude of the fluctuations (characterized by  $\delta$ ) goes to 0. The parameter  $\delta$ , which quantifies the surface disorder, can be related to the constants  $\kappa^*$  and  $\sigma^*$  in the Helfrich model by

$$\delta = \mathbb{E}_{\mathbb{P}} |\nabla h|^2 = \sum_{k \in \mathbb{K}} \frac{1}{\kappa^* |2\pi k|^2 + \sigma^*}. \tag{69}$$

Thus, as  $\kappa^*$  and  $\sigma^*$  increase, the magnitude of the fluctuations decreases, and individual realizations of the surface give rise to isotropic diffusion tensors, the average of which is well approximated by  $\overline{D}_{as}$ .

To verify these two predictions, we approximate  $\overline{D}$  numerically for various parameter values. Realizations of the stationary surface field were generated by sampling the Fourier modes  $\eta_k$  from their respective invariant distribution and performing a fast Fourier transform. For each realization of the surface,  $D(h)$  was computed using the numerical scheme described in Sect. 5.6. In Fig. 6, we plot  $\overline{D}$  for varying bending modulus  $\kappa^*$ , surface tension set to  $\sigma^* = 0, 100$  and  $500$ , and  $K = 32$ . The effect of  $\kappa^*$  and, to a lesser extent  $\sigma^*$  on the variance in the effective diffusion tensor, is clear. We also plot the averaged area scaling approximation for this case. As predicted by Theorem 3 for large values of  $\kappa^*$ , which corresponds to the weak-disorder limit, that is,  $\mathbb{E}_{\mathbb{P}} [|\nabla h|^2] \ll 1$ , the averaged area scaling approximation  $\overline{D}_{as}$  provides a good approximation to  $\overline{D}$ , but as  $\kappa^* \rightarrow 0$ , the disparity between  $\overline{D}$  and  $\overline{D}_{as}$  increases, with  $\overline{D}_{as}$  underestimating the average diffusion tensor.

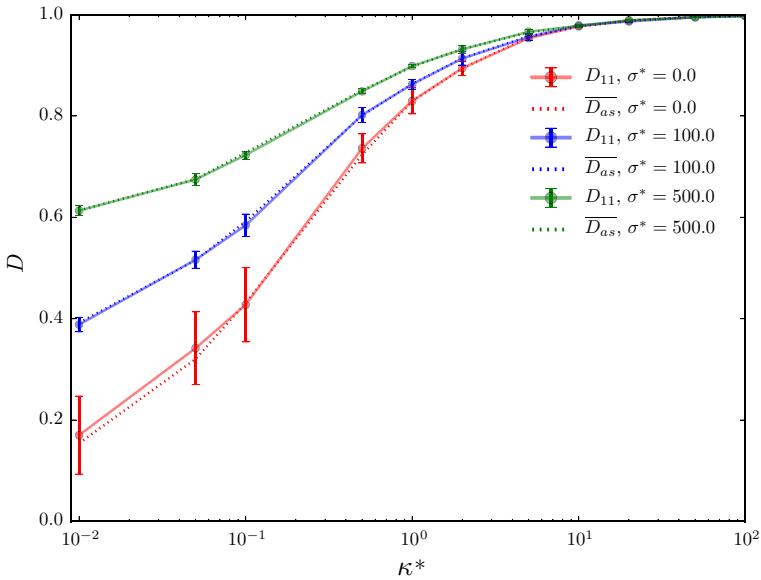


**Fig. 6** Plot of the distributions of the isotropic effective diffusion tensor  $D$  for a quenched realization of a Helfrich surface, with  $K = 32$ , and  $\sigma^* = 0, 100$  and  $100$ . Dots denote the mean of the distribution for each  $\kappa^*$  while error bars denote the standard deviation. The dotted line denotes the average area scaling approximation

### 7 Case II: Diffusion on Surfaces Possessing Purely Temporal Fluctuations

In this section, we study the Case II regime, where the fast-scale fluctuations are entirely temporal, corresponding to  $(\alpha, \beta) = (0, 1)$  in Eq. (29). In Sect. 7.1, we use formal expansions to identify the drift and diffusion tensors of the annealed limit process, which are given by the ergodic averages of the drift and diffusion tensors of the multiscale problem. The subsequent sections will then focus on the Helfrich elastic model where we derive exact and asymptotic expressions for the effective diffusion tensor providing a rigorous justification of the “preaveraging” approximation described in Reister and Seifert (2007), Gustafsson and Halle (1997), Naji and Brown (2007).

#### 7.1 Averaging Result

In this regime, (13) can be written as

$$dX^\varepsilon(t) = F(X^\varepsilon(t), \eta^\varepsilon(t)) dt + \sqrt{2\Sigma(X^\varepsilon(t), \eta^\varepsilon(t))} dB(t), \tag{70a}$$

$$d\eta^\varepsilon(t) = -\frac{1}{\varepsilon} \Gamma \eta^\varepsilon + \sqrt{\frac{2}{\varepsilon}} \Gamma \Pi dW(t), \tag{70b}$$

where  $F$  and  $\Sigma$  are given by (14) and (15), respectively, and where  $B(\cdot)$  is a standard  $d$ -dimensional Brownian motion. The process  $W(\cdot)$  is a standard  $K$ -dimensional

Brownian motion. The generator of the fast process  $\eta^\varepsilon(t)$  is  $\frac{1}{\varepsilon}\mathcal{L}_0$ , with

$$\mathcal{L}_0 f(\eta) = -\Gamma \eta \nabla f(\eta) + \Gamma \Pi : \nabla \nabla f(\eta), \quad f \in C_b^2(\mathbb{R}^d).$$

The fast process  $\eta^\varepsilon(t)$  is geometrically ergodic with invariant distribution  $\mathcal{N}(0, \Pi)$ . In particular,

$$\mathcal{N}[\mathcal{L}_0] = \{\mathbf{1}\} \quad \text{and} \quad \mathcal{N}[\mathcal{L}_0^*] = \{\rho_\eta\},$$

where

$$\rho_\eta(\eta) = \frac{1}{\sqrt{(2\pi)^d |\Pi|}} \exp\left(-\frac{1}{2} \eta \cdot \Pi^{-1} \eta\right), \tag{71}$$

The corresponding backward Kolmogorov equation for this coupled system is given by

$$\frac{\partial v^\varepsilon}{\partial t}(x, \eta, t) = \mathcal{L}^\varepsilon v^\varepsilon(x, \eta, t), \quad (x, \eta, t) \in \mathbb{R}^d \times \mathbb{R}^K \times (0, T] \tag{72a}$$

$$v^\varepsilon(x, \eta, 0) = v(x, \eta), \quad (x, \eta) \in \mathbb{R}^d \times \mathbb{R}^K. \tag{72b}$$

where

$$\mathcal{L}^\varepsilon = \frac{1}{\varepsilon} \mathcal{L}_0 + \mathcal{L}_1, \tag{73}$$

for

$$\mathcal{L}_1 f(x, \eta) = \frac{1}{\sqrt{|g|(x, \eta)}} \nabla_x \cdot \left( \sqrt{|g|(x, \eta)} g^{-1}(x) \nabla_x f(x, \eta) \right).$$

We now state the averaging result for this regime. A formal justification using perturbation expansions is provided in section ‘‘Case II’’ of Appendix. For a rigorous justification, refer to [Duncan \(2013\)](#).

**Theorem 4** *Let  $T > 0$  and suppose that  $\eta^\varepsilon(t)$  is stationary. Then, the process  $X^\varepsilon$  converges weakly in  $C([0, T]; \mathbb{R}^d)$  to a Wiener process  $X^0(t)$ , which is the unique solution of the following Itô SDE:*

$$dX^0(t) = \bar{F}(X^0(t))dt + \sqrt{2\bar{\Sigma}(X^0(t))} dB(t), \tag{74}$$

where

$$\bar{F}(x) = \int_{\mathbb{R}^K} F(x, \eta) \rho_\eta(d\eta) \tag{75}$$

and

$$\bar{\Sigma}(x) = \int_{\mathbb{R}^K} \Sigma(x, \eta) \rho_\eta(d\eta). \tag{76}$$

Moreover, assume that the backward Kolmogorov equation (72a) has initial data  $v$  independent of  $\eta$  such that  $v \in C_b^2(\mathbb{R}^d)$ , then the solution  $v^\varepsilon$  of (72a) converges pointwise to the solution  $v^0$  of the following PDE,

$$\begin{aligned} \frac{\partial v^0}{\partial t}(x, t) &= \bar{F}(x) \cdot \nabla_x v^0(x, t) + \bar{\Sigma}(x) : \nabla_x \nabla_x v^0(x, t), \quad (x, t) \in \mathbb{R}^d \times (0, T] \\ v^0(x, 0) &= v(x), \quad x \in \mathbb{R}^d. \end{aligned}$$

uniformly with respect to  $t$  over  $[0, T]$ . □

### 7.2 Diffusion on a Helfrich Surface in the $(\alpha, \beta) = (0, 1)$ Regime

We can apply Theorem 4 to obtain the annealed limit equations for diffusion on a rapidly fluctuating Helfrich elastic membrane. Indeed, we will show that as  $\varepsilon \rightarrow 0$ , the process  $X(\cdot)$  converges weakly to a pure diffusion process with constant diffusion tensor. To this end, as in Sect. 4, we set  $\mathbb{K} = \{k \in \mathbb{Z}^2 \setminus \{(0, 0)\} \mid |k| \leq c\}$ , and set the coefficients of  $\eta^\varepsilon(t)$  to be

$$\Gamma = \text{diag}(\Gamma_k)_{k \in \mathbb{K}} \text{ and } \Pi = \text{diag}(\Pi_k)_{k \in \mathbb{K}},$$

where  $\Gamma_k$  and  $\Pi_k$  are given by (23) and (24), respectively. For the spatial functions, we choose the standard  $L^2(\mathbb{T}^2)$  Fourier basis  $\{e_k\}_{k \in \mathbb{K}}$  where  $e_k(x) = e^{2\pi i k x}$ . The invariant distribution of  $\eta_k^\varepsilon(t)$  is then given by  $\mu_k = \mathcal{N}(0, \Pi_k)$ .

The form of the limiting equation is strongly dependent on the symmetry properties of the stationary random field.

**Lemma 2** *Let  $h(x)$  be a stationary realization of the random field, that is,*

$$h(x) = \sum_{k \in \mathbb{K}} \eta_k e_k(x),$$

where  $(\eta_k)_{k \in \mathbb{K}} \sim \mu_k$ . Then, for each  $x \in \mathbb{T}^2$ , the vectors

$$(h_{x_1}(x), h_{x_2}(x), h_{x_1 x_2}(x), h_{x_1 x_1}(x)),$$

and

$$(h_{x_1}(x), h_{x_2}(x), h_{x_1 x_2}(x), h_{x_2 x_2}(x)),$$

are both jointly Gaussian with mean zero, and the components of each vector are independent, where  $h_{x_i} = \frac{\partial h(x)}{\partial x_i}$ , for  $x = (x_1, x_2)$ .

*Proof* Since a finite linear combination of centered Gaussian random variables is again a centered Gaussian random variable, it is clear that both vectors are centered Gaussian random vectors. Moreover, the components of each vector are pairwise uncorrelated.

To see this for  $h_{x_1}(x)$  and  $h_{x_2}(x)$

$$\begin{aligned} \mathbb{E} [h_{x_1}(x)h_{x_2}(x)] &= \mathbb{E} \left[ \left( \sum_{k \in \mathbb{K}} (2\pi i k_1) \eta_k e_k(x) \right) \left( \sum_{j \in \mathbb{K}} (2\pi i j_2) \eta_j e_j(x) \right)^* \right] \\ &= (2\pi)^2 \sum_{k \in \mathbb{K}} k_1 k_2 \Pi_k. \end{aligned}$$

Due to the symmetry of  $\mathbb{K}$  around 0, it follows that the term on the RHS is 0, so that  $h_{x_1}(x)$  and  $h_{x_2}(x)$  are uncorrelated. Similar arguments follow for the other pairs of components.

We now state the limit theorem for diffusion on a rapidly fluctuating Helfrich elastic membrane. A formal derivation of formula (77) has been derived in [Naji and Brown \(2007\)](#) and [Reister and Seifert \(2007\)](#).

**Theorem 5** *Let  $T > 0$ , the process  $X(\cdot)$  converges weakly in  $C([0, T]; \mathbb{R}^2)$  to a Brownian motion with scalar diffusion tensor given by*

$$D = \frac{1}{2} \left( 1 + \int_{\mathbb{R}^K} \left[ \frac{1}{|g|(x, \eta)} \right] \rho_\eta(d\eta) \right) \mathbf{I}. \tag{77}$$

Furthermore, the resulting diffusion tensor  $D$  is independent of  $x$ .

*Proof* By Theorem 4, the process  $X(\cdot)$  converges weakly to a process with drift coefficient  $\bar{F}(x)$  and diffusion tensor  $\bar{\Sigma}(x)$  given by (75) and (76), respectively. Consider first the drift coefficient

$$\bar{F}(x) = \int_{\mathbb{R}^K} \left[ \frac{(1 + h_{x_1}^2)h_{x_2x_2} - 2h_{x_1}h_{x_2}h_{x_1x_2} + (1 + h_{x_2}^2)h_{x_1x_1}}{(1 + h_{x_1}^2 + h_{x_2}^2)^2} \begin{pmatrix} h_{x_1} \\ h_{x_2} \end{pmatrix} \right] \rho_\eta(d\eta),$$

Applying Lemma 2, every term in the above sum is an odd function of a centered, Gaussian random vector. Thus, each term equals 0.

Consider now the effective diffusion tensor

$$\bar{\Sigma} = \int_{\mathbb{R}^K} \left[ \frac{1}{1 + h_{x_1}^2 + h_{x_2}^2} \begin{pmatrix} 1 + h_{x_2}^2 & -h_{x_1}h_{x_2} \\ -h_{x_1}h_{x_2} & 1 + h_{x_1}^2 \end{pmatrix} \right] \rho_\eta(d\eta).$$

By the symmetry of  $h_{x_1}$  and  $h_{x_2}$ , the off-diagonal terms are also zero; moreover, the diagonal terms are equal. Thus,

$$\begin{aligned} \int_{\mathbb{R}^K} \left[ \frac{1 + h_{x_2}^2}{1 + h_{x_1}^2 + h_{x_2}^2} \right] \rho_\eta(d\eta) &= \frac{1}{2} \int_{\mathbb{R}^K} \left[ \frac{1 + h_{x_2}^2}{1 + h_{x_1}^2 + h_{x_2}^2} \right] \rho_\eta(d\eta) \\ &\quad + \frac{1}{2} \int_{\mathbb{R}^K} \left[ \frac{1 + h_{x_1}^2}{1 + h_{x_1}^2 + h_{x_2}^2} \right] \rho_\eta(d\eta) \\ &= \frac{1}{2} \left( 1 + \int_{\mathbb{R}^K} \left[ \frac{1}{1 + h_{x_1}^2 + h_{x_2}^2} \right] \rho_\eta(d\eta) \right), \end{aligned}$$

as required. Finally,

$$\begin{aligned} \nabla_x D &= \left[ \int_{\mathbb{R}^K} \nabla_x \left[ \frac{1}{|g|(x, \eta)} \right] \rho_\eta(d\eta) \right] \mathbf{I} \\ &= \left[ -2 \int_{\mathbb{R}^K} \left[ \frac{\nabla_x \nabla_x h(x, \eta) \nabla_x h(x, \eta)}{|g|(x, \eta)^2} \right] \rho_\eta(d\eta) \right] \mathbf{I} = 0, \end{aligned}$$

by the symmetry arguments of Lemma 2, so that  $D$  is independent of  $x$ . □

Besides  $\kappa^*$  and  $\sigma^*$ , the effective diffusion tensor also depends on the ultraviolet cutoff  $c$  (or equivalently  $K$ ). One can observe that

$$\lim_{K \rightarrow \infty} \int_{\mathbb{R}^K} \left[ \frac{1}{|g|(x, \eta)} \right] \rho_\eta(d\eta) = 0,$$

so that for any fixed  $\kappa^*, \sigma^*$ , the effective diffusion  $D$  will approach  $\frac{1}{2}$  as  $K$  approaches  $\infty$ . In fact, for fixed  $K, \sigma^*$  and  $\kappa^*$ , the effective diffusion tensor  $D$  satisfies

$$\frac{1}{2} < D < 1,$$

and recalling that the molecular diffusion tensor  $D_0$  was rescaled to 1, this implies that the diffusion is depleted in the limit of  $\varepsilon \rightarrow 0$ . In the weak-disorder regime (i.e., when  $\mathbb{E} |\nabla h|^2 \ll 1$ ), which corresponds to the large  $\kappa^*$  or large  $\sigma^*$  regime, it is possible to derive estimates for  $D$  by applying Taylor’s theorem and using the fact that  $\nabla h(x)$  is Gaussian to get, as a first-order approximation

$$D = 1 - \frac{1}{2} \delta + O(\delta^{\frac{3}{2}}), \tag{78}$$

where the constant  $\delta$  is related to  $\kappa^*$  and  $\sigma^*$  by (69). Comparing with the corresponding equation for Case I given in (68), we see that, to first order, both regimes exhibit the same behavior in the weak-disorder limit.

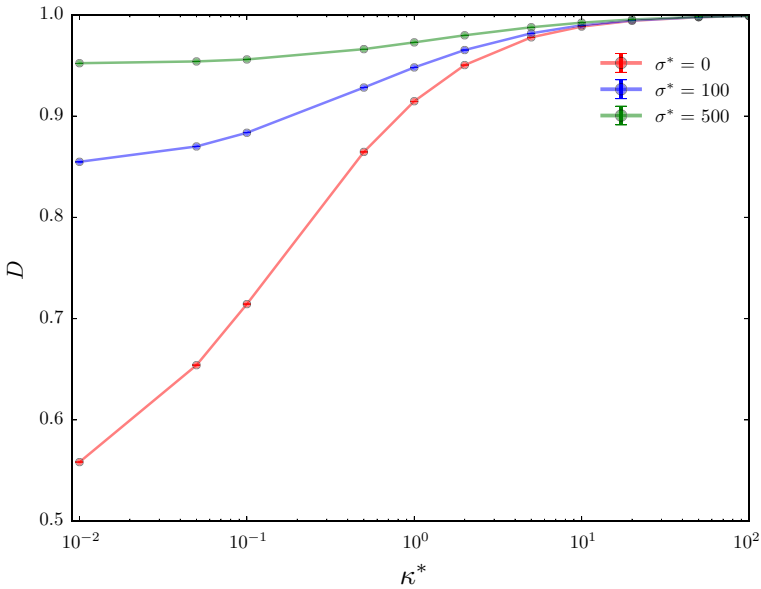


**Fig. 7** Effective diffusion tensor for a diffusion on a fluctuating Helfrich elastic membrane in the  $(\alpha, \beta) = (0, 1)$  scaling for varying  $\kappa^*$  and  $K = 32$

### 7.3 Numerical Examples

We can study how the bending modulus  $\kappa^*$ , surface tension  $\sigma^*$ , and the ultraviolet cutoff  $c$  (or equivalently  $K$ ) affect the effective diffusion tensor numerically. The ensemble average in (76) is computed using a straightforward Monte Carlo method, taking the sample average of  $\frac{1}{|g|(x,\eta)}$  for  $\eta$  sampled from its corresponding stationary measure. As (78) suggests, for small values of  $\kappa^*$  and  $\sigma^*$ , the larger thermal fluctuations of the surface cause a greater reduction in the speed of diffusion of a particle diffusing laterally on the surface. Indeed, one can see that  $(1 - D) \approx \frac{1}{\kappa^*}$  for fixed  $\sigma^*$  and  $(1 - D) \approx \frac{1}{\sigma^*}$  for fixed  $\kappa^*$ . In Fig. 7, we plot  $D$  for varying values of  $\kappa^*$ ,  $K$  and for  $\sigma^* = 0, 100, 500$ . The convergence of  $D$  to  $\frac{1}{2}$  becomes immediately apparent. As expected,  $D$  decays with  $c$ , converging to  $\frac{1}{2}$  as  $c \rightarrow \infty$  (Fig. 8).

### 8 Case III: Diffusion on Surfaces with Comparable Spatial and Temporal Fluctuations

In this section, we consider the Case III regime where  $(\alpha, \beta) = (1, 1)$  in (13). This scaling describes lateral diffusion on a rough surface which is also fluctuating rapidly, but the temporal surface fluctuations occur at a scale commensurate to the characteristic scale of the spatial fluctuations. This scaling was considered for SDEs with periodic spatial and temporal fluctuations in Garnier (1997). A unique characteristic of this scaling regime is that it gives rise to a macroscopic drift term in the limit as  $\varepsilon \rightarrow 0$ ,

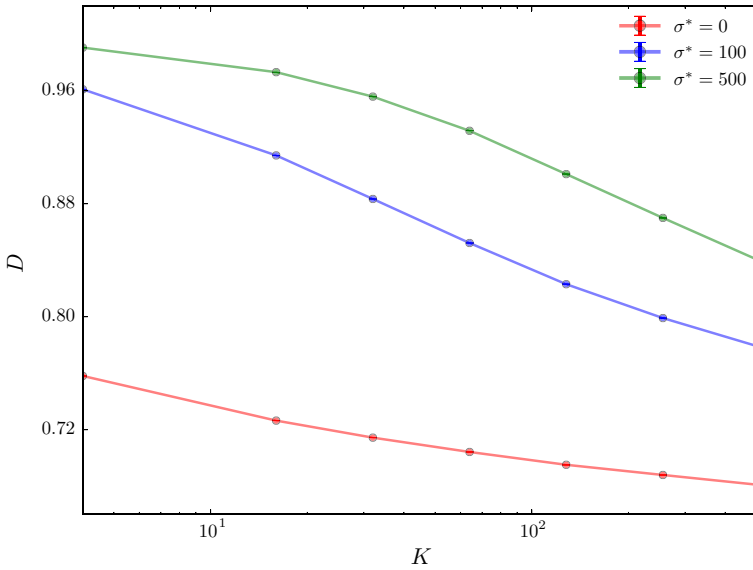


**Fig. 8** Effective diffusion tensor for a diffusion on a fluctuating Helfrich elastic membrane in the (0, 1) scaling for varying  $K$  and  $\kappa^* = 0.1$

which is determined by the rate of change in the corrector  $\chi(y, \eta)$  with respect to the temporal fluctuations.

A similar effective drift term arises in the model considered here. It is not clear that this drift is identically zero in general. However, we identify a natural symmetry condition for the surface fluctuations for which we can prove the effective drift term vanishes. In the remainder of this section, we identify and study the properties of the macroscopic diffusion tensor and provide sufficient conditions for the isotropy of the effective diffusion tensor. Finally, we study the limiting properties of the Helfrich model in this regime.

### 8.1 Homogenization Result

Introducing the fast process  $Y^\varepsilon(t) = \frac{X^\varepsilon(t)}{\varepsilon} \pmod{\mathbb{T}^d}$ , Eq. (29) can be written as fast-slow system

$$dX^\varepsilon(t) = \frac{1}{\varepsilon} F(Y^\varepsilon(t), \eta^\varepsilon(t)) dt + \sqrt{2\Sigma(Y^\varepsilon(t), \eta^\varepsilon(t))} dB(t), \tag{79a}$$

$$dY^\varepsilon(t) = \frac{1}{\varepsilon^2} F(Y^\varepsilon(t), \eta^\varepsilon(t)) dt + \sqrt{\frac{2}{\varepsilon^2} \Sigma(Y^\varepsilon(t), \eta^\varepsilon(t))} dB(t), \tag{79b}$$

$$d\eta^\varepsilon(t) = -\frac{1}{\varepsilon} \Gamma \eta^\varepsilon(t) dt + \sqrt{\frac{2\Gamma\Pi}{\varepsilon}} dW(t), \tag{79c}$$

where  $F$  and  $\Sigma$  are given by (14) and (15), respectively, and where we impose periodic boundary conditions on  $Y^\varepsilon(\cdot)$ . The processes  $B(\cdot)$  and  $W(\cdot)$  are standard  $d$  and  $K$ -

dimensional Brownian motions, respectively. Although the definition of  $Y^\varepsilon(t)$  is only a trivial rescaling of  $X^\varepsilon(t)$  (albeit on a different domain), we include it to make explicit the relationship between the rapidly varying processes  $Y^\varepsilon(t)$  and  $\eta^\varepsilon(t)$ . The infinitesimal generator of the fast process  $Y^\varepsilon(t)$  is given by  $\frac{1}{\varepsilon^2}\mathcal{L}_0$ , where  $\mathcal{L}_0$  is given by

$$\mathcal{L}_0 f(y) = \frac{1}{\sqrt{|g|(y, \eta)}} \nabla_y \cdot \left( \sqrt{|g|(y, \eta)} g^{-1}(y, \eta) \nabla_y f(y) \right), \quad f \in C^2(\mathbb{T}^d). \tag{80}$$

We note that although the spatial and temporal fluctuations appear commensurate in the system of SDEs, the spatial fluctuations relax to equilibrium at a timescale faster than the temporal fluctuations. The limiting equation can thus be considered the result of a reiterated homogenization/averaging problem of the form described in [Bensoussan et al. \(1978, Section 2.11.3\)](#). The limiting equation is thus obtained by homogenizing over  $Y^\varepsilon(t)$  for a frozen value of  $\eta^\varepsilon(t)$  and then averaging over the invariant measure  $\rho_\eta(\cdot)$  of  $\eta^\varepsilon(t)$ .

For  $\eta$  fixed  $\mathcal{L}_0$  satisfies

$$\mathcal{N}[\mathcal{L}_0] = \{\mathbf{1}\} \quad \text{and} \quad \mathcal{N}[\mathcal{L}_0^*] = \{\rho_y(y, \eta)\},$$

where  $\rho_y(y, \eta)$  is given by [\(53\)](#).

As in [Sect. 6](#), for  $\eta \in \mathbb{R}^K$  fixed, we define the corrector  $\chi(y, \eta)$  to be the mean-zero solution of the cell Eq. [\(55\)](#), or equivalently

$$\mathcal{L}_0 \chi(y, \eta) = -F(y, \eta), \quad (y, \eta) \in \mathbb{T}^d \times \mathbb{R}^K. \tag{81}$$

The backward Kolmogorov equation corresponding to the coupled system [\(79\)](#) is given by

$$\frac{\partial v^\varepsilon}{\partial t}(x, y, \eta, t) = \mathcal{L}^\varepsilon v^\varepsilon(x, y, \eta, t), \quad (x, y, \eta, t) \in \mathbb{R}^d \times \mathbb{T}^d \times \mathbb{R}^K \times (0, T] \tag{82a}$$

$$v^\varepsilon(x, y, \eta, 0) = v(x, y, \eta), \quad x \in \mathbb{R}^d \times \mathbb{T}^d \times \mathbb{R}^K. \tag{82b}$$

where

$$\mathcal{L}^\varepsilon = \frac{1}{\varepsilon^2} \mathcal{L}_0 + \frac{1}{\varepsilon} \mathcal{L}_\eta + \frac{1}{\varepsilon} \mathcal{L}_1 + \mathcal{L}_2, \tag{83}$$

for

$$\mathcal{L}_1 f(x, y, \eta) = F(y, \eta) \cdot \nabla_x f(x, y, \eta) + 2\Sigma(y, \eta) : \nabla_x \nabla_y f(x, y, \eta),$$

and

$$\mathcal{L}_2 f(x, y, \eta) = \Sigma(y, \eta) : \nabla_x \nabla_x f(x, y, \eta),$$

and  $\mathcal{L}_\eta$  is the infinitesimal generator of the OU process and is given by

$$\mathcal{L}_\eta f(\eta) = -\Gamma \cdot \nabla_\eta f(\eta) + \Gamma \Pi : \nabla_\eta \nabla_\eta f(\eta). \tag{84}$$

The following theorem states the homogenization result for this scaling. A formal justification will be given in section “Case III” of Appendix. A rigorous proof using probabilistic methods can be found in Duncan (2013). As in the previous chapters, we use the convention that  $(\nabla_y \chi)_{ij} = \frac{\partial \chi^{e_i}}{\partial y_j}$ .

**Theorem 6** *Let  $0 < \varepsilon \ll 1$  and  $T = \mathcal{O}(1)$ , and suppose  $\eta^\varepsilon(t)$  is stationary. Then, as  $\varepsilon \rightarrow 0$ , the process  $X^\varepsilon(\cdot)$  converges weakly in  $C([0, T]; \mathbb{R}^d)$  to  $X^0$ , which is a weak solution of the following Itô SDE*

$$dX^0(t) = V dt + \sqrt{2D} dB(t), \tag{85}$$

where the effective diffusion tensor  $D$  is equal to  $D_1$  given by (54), that is,

$$D = \int_{\mathbb{R}^K} \int_{\mathbb{T}^d} (I + \nabla_y \chi) g^{-1}(y, \eta) (I + \nabla_y \chi)^\top \rho_y(y, \eta) \rho_\eta(\eta) dy d\eta, \tag{86}$$

and the effective drift term  $V$  is given by

$$V = \int_{\mathbb{R}^K} \int_{\mathbb{T}^d} \mathcal{L}_\eta \chi \rho_y(y, \eta) \rho_\eta(\eta) dy d\eta. \tag{87}$$

Moreover, if the backward Eq. (82a) has initial data  $v$ , independent of the fast process, such that  $v \in C_b^2(\mathbb{R}^d)$ , then the solution  $v^\varepsilon$  of (82a) converges pointwise to the solution  $v_0$  of

$$\begin{aligned} \frac{\partial v^0}{\partial t}(x, t) &= V \cdot \nabla_x v^0(x, t) + D : \nabla_x \nabla_x v^0(x, t), & (x, t) \in \mathbb{R}^d \times (0, T], \\ v^0(x, 0) &= v(x), & x \in \mathbb{R}^d. \end{aligned} \tag{88}$$

uniformly with respect to  $t$  over  $[0, T]$ . □

### 8.2 Properties of the Effective Diffusion Process

Comparing the effective behavior of the homogenized diffusion processes in Case I and Case III, we see that the introduction of fast temporal fluctuations gives rise to a time-averaging of the effective diffusion tensor  $D$ , so that the effective diffusion in the  $(\alpha, \beta) = (1, 1)$  case is equal to the averaged effective diffusion tensor  $D_1$  for diffusion on a surface with quenched fluctuations, as described in Sect. 6. Thus, all the properties of the effective diffusion tensor hold identically in this case. The following proposition summarizes the most important properties.

**Proposition 5** *Let  $D$  be the effective diffusion given by (86), then*

- (i)  $D$  is a strictly positive definite matrix.

(ii) In particular, for a unit vector  $e \in \mathbb{R}^d$

$$0 < \overline{D}_* \leq e \cdot De \leq \overline{D}^* \leq 1, \tag{89}$$

where  $\overline{D}^* = \mathbb{E} [D^*(h)]$  and  $\overline{D}_* = \mathbb{E} [D_*(h)]$ , for  $D^*$  and  $D_*$  given by (44) and (43), respectively, and where  $\mathbb{E} [\cdot]$  denotes expectation with respect to the invariant measure of  $\eta^\varepsilon(t)$ .

(iii) For  $d = 2$ , if the condition of Proposition 4 holds, then  $D$  is isotropic.

(iv) If additionally  $\mathbb{E} [|\nabla h(x)|^2] = \delta \ll 1$ , then

$$D = \overline{D}_{as} + O(\delta^2),$$

where  $\overline{D}_{as} = \mathbb{E} \left[ \frac{1}{Z(h)} \right]$ . □

We turn our attention to the effective drift term  $V$  given by (86). Unlike  $D$ , the effective drift depends on  $\chi(y, \eta)$ , which is only unique up to a constant depending on  $\eta$ . However, for any function  $c(\eta)$ , we have that

$$\begin{aligned} \int \int_{\mathbb{T}^d} \mathcal{L}_\eta c(\eta) \rho_y(y, \eta) \rho_\eta(\eta) dy d\eta &= \int \mathcal{L}_\eta c(\eta) \left( \int_{\mathbb{T}^d} \rho_y(y, \eta) dy \right) \rho_\eta(\eta) d\eta \\ &= \int \mathcal{L}_\eta c(\eta) \rho_\eta(\eta) d\eta = 0, \end{aligned}$$

since  $\int_{\mathbb{T}^d} \rho_y(y, \eta) dy = 1$  for all  $\eta$ . It follows that the effective drift  $V$  is uniquely defined independent of any additive terms independent of  $y$ .

The fact that a macroscopic drift  $V$  arises in this scaling regime is surprising. While numerical simulations suggest that  $V$  is always zero, we have not been able to prove this in general. However, we can show that it is true for surfaces that satisfy the following natural symmetry condition. Suppose there exists a linear orthogonal map  $\mathcal{C} : \mathbb{R}^K \rightarrow \mathbb{R}^K$  which commutes with  $\Pi$  and  $\Gamma$  (in particular  $\rho_\eta$  is invariant with respect to  $\mathcal{C}$ ) such that

$$h(x, \mathcal{C}^\perp \eta) = h(x^\perp, \eta), \tag{90}$$

where  $x_i^\perp = 1 - x_i$  for  $i \in \{1, \dots, d\}$ , or equivalently that

$$\mathcal{C} e(x) = e(x^\perp),$$

where  $e(x) = \{e_k(x)\}_{k \in \mathbb{K}}$ .

Condition (90) arises naturally in the case where  $e_k$  are the Fourier basis for the Laplacian on  $[0, 1]^2$ . The surface perturbation  $h$  can then be rewritten as

$$h(x, \eta) = \sum_{k \in \mathbb{K}_{\text{even}}} \eta_k^e e_k^e(x) + \sum_{k \in \mathbb{K}_{\text{odd}}} \eta_k^o e_k^o(x),$$

where  $e_k^e$  and  $e_k^o$  are, respectively, even and odd functions on  $[0, 1]^2$  for all  $k \in \mathbb{K}$ . If  $\mathcal{C}$  is the diagonal matrix defined by

$$\mathcal{C}^\top \eta = \mathcal{C}^\top (\eta^e, \eta^o) = (\eta^e, -\eta^o),$$

for  $\eta^e = (\eta_k^e)_{k \in \mathbb{K}_{\text{even}}}$  and  $\eta^o = (\eta_k^o)_{k \in \mathbb{K}_{\text{odd}}}$ , we see that condition (90) is trivially satisfied. We can show the following result.

**Proposition 6** *Suppose (90) holds, then the effective drift  $V$  equals  $\mathbf{0}$ .*

*Proof* We first note that (90) implies that

$$g^{-1}(x, \mathcal{C}\eta) = g^{-1}(x^\perp, \eta),$$

and

$$|g|(x, \mathcal{C}\eta) = |g|(x^\perp, \eta).$$

Consider the cell equation for the corrector  $\chi^e(y, \eta)$  given by

$$\nabla \cdot \left( \sqrt{|g|(y, \eta)} g^{-1}(y, \eta) (\nabla \chi^e(y, \eta) + e) \right) = 0.$$

Making the substitution  $\eta \rightarrow \mathcal{C}\eta$ , then using the relations for  $g^{-1}$  and  $|g|$  and changing variables in  $y$ , we have

$$-\nabla \cdot \left( \sqrt{|g|(y, \eta)} g^{-1}(y, \eta) (-\nabla \tilde{\chi}^e(y, \eta) + e) \right) \Big|_{y=y^\perp} = 0, \tag{91}$$

where  $\tilde{\chi}^e(y, \eta) = \chi^e(y^\perp, \mathcal{C}\eta)$ . It follows that

$$\chi^e(y^\perp, \mathcal{C}\eta) = -\chi^e(y, \eta). \tag{92}$$

Applying (91) and using the fact that  $\mathcal{C}$  commutes with  $\Gamma$  and  $\Pi$ , we obtain

$$\begin{aligned} -\mathcal{L}_\eta \chi^e(y^\perp, \eta) &= -\Gamma \eta \cdot \mathcal{C} \nabla_\eta \chi^e(y, \mathcal{C}^\top \eta) + \mathcal{C}^\top \Gamma \Pi \mathcal{C} : \nabla \nabla \chi^e(y, \mathcal{C}^\top \eta) \\ &= -\Gamma \mathcal{C}^\top \eta \cdot \nabla_\eta \chi^e(y, \mathcal{C}^\top \eta) + \Gamma \Pi : \nabla \nabla \chi^e(y, \mathcal{C}^\top \eta) \\ &= \mathcal{L}_\eta \chi^e(y, \mathcal{C}^\top \eta). \end{aligned}$$

Using the invariance of  $\rho_y$  with respect to  $\mathcal{C}$ , the effective drift term  $V$  will then be given by

$$\begin{aligned} V &= \int_{\mathbb{T}^d} \int_{\mathbb{T}^d} \mathcal{L}_\eta \chi^e(y^\perp, \eta) \rho_y(y^\perp, \eta) \rho_\eta(\eta) \, dy \, d\eta \\ &= - \int_{\mathbb{T}^d} \int_{\mathbb{T}^d} \mathcal{L}_\eta \chi^e(y, \mathcal{C}^\top \eta) \rho_y(y, \mathcal{C}^\top \eta) \rho_\eta(\eta) \, dy \, d\eta \\ &= -V, \end{aligned}$$

proving the result. □

As an example, we can consider the model for a thermally excited Helfrich surface in the  $(\alpha, \beta) = (1, 1)$  scaling. It follows from Proposition 5 that the effective diffusion tensor is isotropic. Moreover, since the conditions of Proposition 6 hold, the effective drift is  $\mathbf{0}$ . It follows that the diffusion process  $X^\varepsilon(t)$  converges to a Brownian motion on  $\mathbb{R}^2$  with a scalar diffusion tensor  $D$ . As the effective diffusion  $D$  is equal to the effective diffusion tensor  $D_1$  of Sect. 6.1, the dependence of  $D_1$  on the parameters  $\kappa^*$ ,  $\sigma^*$  and  $K$  hold equivalently.

**9 Case IV: Diffusion on Surfaces with Temporal Fluctuations Faster than Spatial Fluctuations**

In this section, we consider the  $(\alpha, \beta) = (1, 2)$  scaling. In this scaling, the surface possesses rapid spatial and temporal fluctuations but the temporal fluctuations are much faster than the spatial fluctuations. Writing  $Y^\varepsilon(t) := \frac{X^\varepsilon(t)}{\varepsilon} \bmod \mathbb{T}^d$  the fast–slow system for this regime is given by

$$dX^\varepsilon(t) = \frac{1}{\varepsilon} F(Y^\varepsilon(t), \eta^\varepsilon(t)) dt + \sqrt{2\Sigma(Y^\varepsilon(t), \eta^\varepsilon(t))} dB(t), \tag{93a}$$

$$dY^\varepsilon(t) = \frac{1}{\varepsilon^2} F(Y^\varepsilon(t), \eta^\varepsilon(t)) dt + \sqrt{\frac{2}{\varepsilon^2} \Sigma(Y^\varepsilon(t), \eta^\varepsilon(t))} dB(t), \tag{93b}$$

$$d\eta^\varepsilon(t) = -\frac{1}{\varepsilon^2} \Gamma \eta^\varepsilon(t) + \sqrt{\frac{2\Gamma\Pi}{\varepsilon^2}} dW(t), \tag{93c}$$

where  $B(\cdot)$  is a standard  $d$ -dimensional Brownian motion, and  $W(\cdot)$  is a standard  $K$ -dimensional Brownian motion. As in Sect. 8, the process  $Y^\varepsilon(t)$  is introduced to make explicit the relationship between the rapidly varying processes  $Y^\varepsilon(t)$  and  $\eta^\varepsilon(t)$ . The infinitesimal generator of the underlying fast process is given by  $\frac{1}{\varepsilon^2} \mathcal{G}$  where

$$\mathcal{G} f(y, \eta) = (\mathcal{L}_0 + \mathcal{L}_\eta) f(y, \eta), \quad f \in C_c^2(\mathbb{T}^d \times \mathbb{R}^K),$$

where  $\mathcal{L}_0$  and  $\mathcal{L}_\eta$  are given by (80) and (84), respectively.

Unlike in the previous cases, it is not immediately clear that the fast process is geometrically ergodic, i.e., that the fast process converges exponentially fast to a unique invariant measure. Moreover, due to the unbounded support of the surface fluctuations, the infinitesimal generator is no longer uniformly elliptic. Thus, we cannot apply standard elliptic theory to obtain a Fredholm alternative for this operator. In Proposition 7, we prove the geometric ergodicity of the fast process. The proof is a straightforward application of the results in Mattingly et al. (2002), Mattingly and Stuart (2002), which are based on the results of the classical Meyn and Tweedie theory (Meyn and Tweedie 2009). In Proposition 7, we show that there exists a unique, smooth solution of the Poisson problem for this scaling regime, provided the centering equation holds.

### 9.1 Homogenization Result

We first identify the fast process  $(Y^\varepsilon(t), \eta^\varepsilon(t))$  as a rescaling of a  $\mathbb{T}^d \times \mathbb{R}^K$ -valued process independent of  $\varepsilon$ . Indeed, define  $(Y(t), \eta(t))$  as follows:

$$dY(t) = F(Y(t), \eta(t))dt + \sqrt{2\Sigma(Y(t), Z(t))} d\hat{B}(t), \tag{94a}$$

$$d\eta(t) = -\Gamma\eta(t) + \sqrt{2\Gamma\Pi}d\hat{W}(t), \tag{94b}$$

where  $\hat{B}(t)$  is a standard  $\mathbb{R}^d$ -valued Brownian motion,  $\hat{W}(t)$  is a standard  $\mathbb{R}^K$ -valued Brownian motion. The joint process  $(Y(t), \eta(t))$  has infinitesimal generator  $\mathcal{G}$ . It is straightforward to show that the following equality holds (in law),

$$(Y^\varepsilon(t), \eta^\varepsilon(t)) = \left( Y(t/\varepsilon^2), \eta(t/\varepsilon^2) \right).$$

**Proposition 7** *The process  $(Y(t), \eta(t))$  possesses a unique invariant measure  $\rho$  with smooth, positive density with respect to the Lebesgue measure on  $\mathbb{T}^d \times \mathbb{R}^K$ , which is the unique normalizable solution of*

$$\mathcal{G}^* \rho = 0. \tag{95}$$

Let  $P_t$  be the Markov semigroup corresponding to  $(Y(t), \eta(t))$ . Then, there exists a constant  $\mu \in (0, 1)$  such that for all functions  $f : \mathbb{T}^d \times \mathbb{R}^K \rightarrow \mathbb{R}$ , such that

$$|f|(y, \eta) \leq CU(\eta), \quad (y, \eta) \in \mathbb{T}^d \times \mathbb{R}^K, \tag{96}$$

where

$$U(\eta) := (1 + |\eta|^2) \tag{97}$$

the following estimate holds

$$\left| \mathbb{E}^{(y_0, \eta_0)} f(Y(t), \eta(t)) - \int f(y, \eta) \rho(dy, d\eta) \right| \leq C'U(\eta_0)e^{-\mu t}, \tag{98}$$

where  $\mathbb{E}^{(y_0, \eta_0)}$  denotes expectation conditioned on  $(Y(0), \eta(0)) = (y_0, \eta_0) \in \mathbb{T}^d \times \mathbb{R}^K$ . In particular, this implies that

$$\left\| P_t f - \int f(y, \eta) \rho(dy, d\eta) \right\|_{L^2(\rho)} \leq C''e^{-\mu t}, \tag{99}$$

for some positive constants  $C', C''$ .

For this scaling regime, the Poisson problem takes the form

$$\mathcal{G}\chi(y, \eta) = -F(y, \eta), \quad (y, \eta) \in \mathbb{T}^d \times \mathbb{R}^K. \tag{100}$$

The existence of a smooth solution  $\chi$  to (100) is guaranteed by the following result.

**Proposition 8** *Suppose the following centering assumption holds*

$$\int_{\mathbb{T}^d \times \mathbb{R}^K} F(y, \eta) \rho(dy, d\eta) = 0. \tag{101}$$

Then, there exists a unique, smooth solution  $\chi \in D(\mathcal{G})$  such that

$$\int_{\mathbb{T}^d \times \mathbb{R}^K} \chi(y, \eta) \rho(dy, d\eta) = 0$$

which solves (100). The solution  $\chi$  satisfies

$$|\chi(y, \eta)| \leq C(1 + |\eta|^2), \quad (y, \eta) \in \mathbb{T}^d \times \mathbb{R}^K$$

where  $C > 0$  is a constant independent of  $(y, \eta)$ . Moreover,

$$\begin{aligned} & \int \nabla_y \chi^\top g^{-1} \nabla_y \chi \rho(dy, d\eta) + \int \nabla_\eta \chi(y, \eta)^\top \Gamma \Pi \nabla_\eta \chi(y, \eta) \rho(dy, d\eta) \\ & = -2 \int \chi(y, \eta) \otimes \mathcal{G} \chi(y, \eta) \rho(dy, d\eta) < \infty. \end{aligned} \tag{102}$$

□

As before, the backward Kolmogorov equation corresponding to (93) is given by

$$\frac{\partial v^\varepsilon}{\partial t}(x, y, \eta, t) = \mathcal{L}^\varepsilon v^\varepsilon(x, y, \eta, t), \quad (x, y, \eta, t) \in \mathbb{R}^d \times \mathbb{T}^d \times \mathbb{R}^K \times (0, T] \tag{103a}$$

$$v^\varepsilon(x, 0) = v(x), \tag{103b}$$

where

$$\mathcal{L}^\varepsilon = \frac{1}{\varepsilon^2} \mathcal{G} + \frac{1}{\varepsilon} \mathcal{L}_1 + \mathcal{L}_2 \tag{104}$$

for

$$\begin{aligned} \mathcal{L}_1 f(x, y, \eta) &= \frac{1}{\sqrt{|g|}(y, \eta)} \nabla \cdot \left( \sqrt{|g|}(y, \eta) g^{-1}(y, \eta) \right) \cdot \nabla_x f(x, y, \eta) \\ & \quad + 2g^{-1}(y, \eta) : \nabla_x \nabla_y f(x, y, \eta), \end{aligned}$$

and

$$\mathcal{L}_2 f(x, y, \eta) = g^{-1}(y, \eta) : \nabla_x \nabla_x f(x, y, \eta).$$

We assume that the initial condition  $v$  is independent of the fast processes. Having Propositions 7 and 8, we can state the homogenization result for this regime. As in the previous cases, we provide a formal derivation based on multiscale expansions in section “Case IV” of Appendix and refer interested readers to Duncan (2013) for a rigorous proof, based on the central limit theorem for additive functionals of Markov processes Komorowski et al. (2012).

**Theorem 7** *Suppose Assumption (101) holds and  $\eta^\varepsilon(t)$  is stationary. Then, as  $\varepsilon \rightarrow 0$ , the process  $X^\varepsilon(\cdot)$  converges weakly in  $C([0, T]; \mathbb{R}^d)$  to a Brownian motion with diffusion tensor  $D$  given by*

$$D = \int (I + \nabla_y \chi) g^{-1} (I + \nabla_y \chi)^\top \rho(dy, d\eta) + \int \nabla_\eta \chi \Gamma \Pi \nabla_\eta \chi^\top \rho(dy, d\eta). \tag{105}$$

Moreover, if the backward Eq. (103a) has initial data  $v$ , independent of  $\varepsilon$  such that  $v \in C_b^2(\mathbb{R}^d)$ , then the solution  $v^\varepsilon$  of (103a) converges pointwise to the solution  $v_0$  of

$$\frac{\partial v^0}{\partial t}(x, t) = D : \nabla_x \nabla_x v^0(x, t), \quad (x, t) \in \mathbb{R}^d \times (0, T] \tag{106a}$$

$$v^0(x, 0) = v(x), \quad x \in \mathbb{R}^d, \tag{106b}$$

uniformly with respect to  $t$  over  $[0, T]$ . □

Due to the lack of an explicit invariant measure for the fast process, it is not clear whether or not the centering condition holds. Numerical experiments suggest that the centering condition does hold for the surfaces we consider; however, it is not clear that this holds in general. If the centering condition is not satisfied, then one can consider the effective behavior of the process  $X^\varepsilon(t)$  close to where the mean drift  $V't$  has taken it, where

$$V' = \int_{\mathbb{T}^d \times \mathbb{R}^K} F(y, \eta) \rho(dy, d\eta).$$

Indeed, we can show that the process  $X^\varepsilon(t) - \frac{V't}{\varepsilon}$  converges to a Brownian motion for small  $\varepsilon$  (Pavliotis et al. 2007).

For surfaces that satisfy the symmetric condition given by (90), we are able to show that the centering condition holds. The proof is very similar to that of Proposition 6 and is omitted.

**Proposition 9** *Assume that condition (90) is satisfied, then the centering condition (101) holds.* □

### 9.2 Numerical Experiments

Rather than resort to direct numerical simulations of the coupled SDEs, we instead use a finite element scheme to solve the equations for the invariant measure and the

corrector. The finite element approximation then becomes  $K+2$ -dimensional problem. For the sake of tractability, we restrict our interest to when  $d = 2$  and  $K = 1$ . We calculate  $D$  numerically as follows:

1. We construct a piecewise linear finite element approximation to Eq. (95) on a regular, triangulated mesh of the domain

$$\Omega_M = \{(y_1, y_2, \eta) \in [0, 1] \times [0, 1] \times [-M, M]\},$$

where  $M$  is chosen so that the support of  $\rho$  outside  $[-M, M]$  is small. We impose periodic boundary conditions on the boundaries in the  $y_1$  and  $y_2$  directions, and no-flux boundary conditions in the  $\eta$  direction.

2. The solution  $\rho$  of (95) is then obtained by solving the corresponding generalized eigenvalue problem for the eigenvector corresponding to the zero eigenvalue. The resulting eigenvector is then normalized over  $\Omega_M$  to give an approximation to  $\rho$ .
3. The components of the corrector are computed by solving the Poisson Eq. (100) using a piecewise linear finite element scheme on the same mesh.
4. Finally, the components of the effective diffusion tensor are computed by integrating (105) using standard quadrature over  $\Omega_M$ .

We apply the above steps to compute the effective diffusion tensor for the surface given by  $h(x, \eta(t))$  where

$$h(x, \eta) = \eta \sin(2\pi x) \sin(2\pi y), \tag{107}$$

and  $\eta(t)$  is an OU process with SDE

$$d\eta(t) = -\Gamma \eta(t) dt + \sqrt{2\Gamma} \Pi W(t),$$

where  $\Gamma = \frac{\kappa^* |2\pi k|^4 + \sigma^* |2\pi k|^2}{|2\pi k|^2}$ ,  $\Pi = \frac{1}{\kappa^* |2\pi k|^4 + \sigma^* |2\pi k|^2}$ , and where  $k = (1, 1)^\top$ .

In Fig. 9, we plot the components of  $D$  for  $\kappa^* \in [10^{-3}, 1.0]$ . We note immediately that the symmetry in  $h(x, \eta)$  is sufficient to ensure that  $D$  is isotropic. Moreover, as in the previous macroscopic limits being considered,  $D$  appears to be bounded above by 1, so that the macroscopic diffusion is depleted with respect to the molecular diffusion tensor.

### 10 Other Distinguished Limits

The four cases considered in this paper are not exhaustive, and indeed, for any  $\alpha$  and  $\beta$ , one can use a similar approach to derive a well-defined limit. While not every choice of  $(\alpha, \beta)$  will give rise to a limiting SDE without further assumptions, in the particular case of lateral diffusion on a Helfrich surface, the limiting equations can be described very succinctly.

By relabeling  $\varepsilon^\alpha$  as  $\varepsilon$ , we need only consider the regimes  $(\alpha, \beta) = (0, 1)$  and  $(\alpha, \beta) \in \{1\} \times [-\infty, \infty)$ . If we denote by  $D_1(\eta)$ ,  $D_2$ ,  $D_3$  and  $D_4$ , the effective diffusion tensors given by (40), (77), (86), and (105), respectively, corresponding

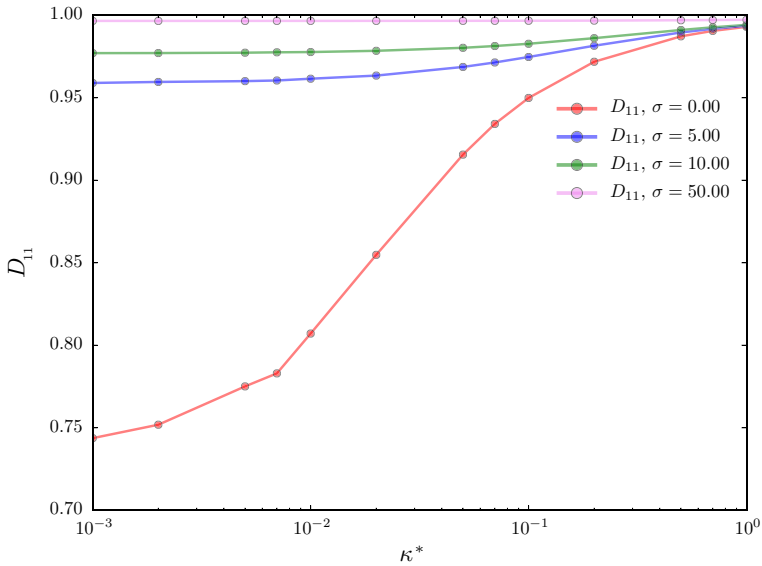


**Fig. 9** Plots of the  $D_{1,1}$  component of the effective diffusion tensor for the surface given by (107) in the  $(\alpha, \beta) = (1, 2)$  regime

**Table 1** Distinguished limits for the system  $(X^\varepsilon(t), \eta^\varepsilon(t))$  describing the evolution of a particle diffusion on a Helfrich elastic surface undergoing thermal fluctuations

| Scaling regime                        | Macroscopic limit                   |
|---------------------------------------|-------------------------------------|
| $\alpha = 0, \beta = 1,$              | $X^0(t) = \sqrt{2D_2}B(t)$          |
| $\alpha = 1, -\infty \leq \beta < 0,$ | $X^0(t) = \sqrt{2D_1(\eta(0))}B(t)$ |
| $\alpha = 1$ and $\beta = 0,$         | $X^0(t) = \sqrt{2D_1(\eta(t))}B(t)$ |
| $\alpha = 1$ and $0 < \beta < 2,$     | $X^0(t) = \sqrt{2D_3}B(t)$          |
| $\alpha = 1$ and $\beta = 2,$         | $X^0(t) = \sqrt{2D_4}(t)$           |
| $\alpha = 1$ and $2 < \beta \leq 3,$  | Not determined                      |
| $\alpha = 1$ and $\beta > 3,$         | $X^0(t) = \sqrt{2D_2}B(t)$          |

to Case I to IV, then one can show that the process  $X^\varepsilon(t)$  will converge weakly in  $C([0, T]; \mathbb{R}^d)$  to a process  $X^0(t)$  as defined in Table 1.

The justification of this result can be found in Duncan (2013) where a probabilistic approach similar to Garnier (1997) is adopted. To prove the weak convergence of  $X^\varepsilon(t)$  to  $X^0(t)$  as  $\varepsilon \rightarrow 0$ , we use Itô’s formula and the solution of an auxiliary PDE to decompose each singular drift into a sum of a martingale and a number of “remainder” drift terms. While some of these remainder terms may also be singular, they are of lower order, and this process may be iterated until  $X^\varepsilon(t)$  has been decomposed into a sum of martingale terms and remainder terms that are  $O(1)$  with respect to  $\varepsilon$ . The result then follows by the martingale central limit theorem.

When applying this approach to the  $\alpha = 1, 2 < \beta \leq 3$  regime, it is not clear whether the auxiliary PDEs that arise are well posed. By the Fredholm alternative, existence of a solution depends on a solvability condition, which is not satisfied in general for the fluctuating Helfrich surface. Thus, it does not appear possible to remove

the singular drift terms that arise in this regime, so that a well-defined limit will not exist as  $\varepsilon \rightarrow 0$ .

As can be seen, the different effective behavior can be broadly split into three separate classes depending on the relative speed of the spatial and temporal fluctuations. For  $\beta \leq 0$ , the fast fluctuations are contributed entirely by the small-scale spatial structure of the surface and no averaging over the fluctuating surface modes occurs. This regime can thus be considered to be a trivial extension of the macroscopic limit derived in Case I. If the relaxation time of the Fourier modes is comparable with the timescale of the lateral diffusion process, then the effective diffusion tensor will depend on the current state  $\eta(t)$  of the surface. If the surface is fluctuating at an much shorter timescale, then, at the  $O(1)$  timescale, the surface is quenched and the effective diffusion tensor will depend only on the initial surface configuration.

For  $0 < \beta < 2$ , the OU process will relax to equilibrium sufficiently fast for averaging to occur at  $O(1)$  scales. At an  $O(\frac{1}{\varepsilon})$  timescale, the process will have homogenized over the spatial fluctuations for a “frozen” surface configuration. At the  $O(1)$  timescale, additional averaging will take place due to temporal fluctuations. The effective diffusion tensor  $D_3$  will be the spatially homogenized diffusion tensor  $D_1(\eta)$  averaged over the invariant measure of  $\eta(t)$ , as was described in Case III.

For  $\beta > 3$ , the rapid temporal fluctuations dominate the fast process, and the diffusion process will have been averaged over the surface Fourier modes even at the characteristic timescale of the rapid spatial fluctuations. Thus, over macroscopic timescales, the diffusion process is well approximated by its annealed disorder limit, as in Case II for  $(\alpha, \beta) = (0, 1)$ .

## 11 Conclusion

We have studied a model for the diffusion of particles on a rough, rapidly fluctuating quasi-planar surface where the surface is periodic in space and with temporal fluctuations modelled by a stationary, ergodic Markovian process. By considering the coupled system of particle diffusion and surface fluctuations, we identified a natural set of distinguished limits that arise from different relationships between the spatial and temporal fluctuations. Through the application of multiscale expansions, we thus provided a unified approach to studying the macroscopic effects of both rapid spatial and temporal fluctuations on a laterally diffusing particle. We identified four natural scaling regimes that possess interesting limiting behavior and in each case identified which properties of the surface fluctuations have a dominant effect on the macroscopic diffusion tensor.

The regimes described in Case I and Case II have previously been considered in [Gustafsson and Halle \(1997\)](#) and [Naji and Brown \(2007\)](#) to study diffusion on quenched and annealed Helfrich fluctuating membranes, respectively. Using multiscale analysis techniques, we rederived the main results in each of these papers and recovered bounds that had been previously obtained heuristically. After making explicit the fact that these two cases correspond to different scalings of the same model, we then consider other possible scalings limits for this model, namely Case III and Case IV as examples of scalings containing both rapid spatial and temporal fluctuations. We believe that this work provides a clear unified approach to the problem

of lateral diffusion on rapidly varying surfaces, bringing together previously derived results in a single framework that can be analyzed with a common set of methods.

While the effective diffusion and drift coefficients do not always have closed forms, we identified natural symmetry assumptions that guarantee that the effective diffusion has an explicit expression depending only on the surface area. Moreover, we derive bounds of varying degrees of tightness that are satisfied by the effective diffusion tensor for general surfaces. To illustrate the derived results, numerical schemes which compute the effective diffusion tensor using finite elements were implemented.

As noted in [Naji and Brown \(2007\)](#), for the fluctuating Helfrich elastic membrane model, the measured diffusion tensor will deviate significantly from the effective diffusion tensor when the small-scale parameter  $\varepsilon$  is not small. In such cases, the multiscale approach can still be applicable in these regimes by computing higher-order correctors ([Pavliotis and Stuart 2008](#); [Bensoussan et al. 1978](#)) that quantify the disparity between the multiscale process and the homogenized process in terms of powers of  $\varepsilon$ .

The model presented in this paper can be extended in several directions. It would be interesting to consider extensions of this problem such as curvature-coupled diffusion [similar to the models presented in [Reister and Seifert \(2007\)](#), [Leitenberger et al. \(2008\)](#), [Reister-Gottfried et al. \(2010\)](#)] or diffusion on membranes with nonthermal fluctuations, such as [Lin et al. \(2006\)](#). Furthermore, it would be interesting to extend the approach to study more general surfaces, where a curved manifold is perturbed by rapid normal fluctuations, and possibly extending this to the case of closed surfaces embedded in  $\mathbb{R}^3$ , which to our knowledge has not been previously considered analytically.

**Acknowledgments** A.D. is grateful to EPSRC for financial support and thanks to the Centre for Scientific Computing @ Warwick for computational resources. G.P. acknowledges financial support from EPSRC Grant Nos. EP/J009636/1 and EP/H034587/1. A.M.S. is grateful to EPSRC and ERC for financial support.

## 12 Appendix: Formal Multiscale Expansions

In this section, we formally derive the limiting equations in each of the scaling regimes using multiscale expansions.

### 12.1 Case I

To derive the homogenized equation in this regime, we make the ansatz that the solution  $v^\varepsilon$  of (35) is of the form

$$v^\varepsilon = v_0(x, y, t) + \varepsilon v_1(x, y, t) + \varepsilon^2 v_2(x, y, t) + \dots, \tag{108}$$

for smooth  $v_i : \mathbb{R}^d \times \mathbb{T}^d \times [0, T] \rightarrow \mathbb{R}^d$ . Substituting (108) in (35) and identifying equal powers of  $\varepsilon$ , we obtain the following equations

$$O\left(\frac{1}{\varepsilon^2}\right) : \mathcal{L}_0 v_0(x, y, t) = 0, \tag{109}$$

$$O\left(\frac{1}{\varepsilon}\right) : \mathcal{L}_0 v_1(x, y, t) = -\mathcal{L}_1 v_0(x, y, t), \tag{110}$$

$$O(1) : \mathcal{L}_0 v_2(x, y, t) = \frac{\partial v_0}{\partial t} - \mathcal{L}_1 v_1(x, y, t) - \mathcal{L}_2 v_0(x, y, t), \tag{111}$$

for  $(x, y, t) \in \mathbb{R}^d \times \mathbb{T}^d \times (0, T]$ .

Since the nullspace of  $\mathcal{L}_0$  contains only constants in  $y$ , Eq. (109) thus implies that  $v_0$  is a function of  $x$  and  $t$  only. Equation (110) becomes

$$\mathcal{L}_0 v_1(x, y, t) = -F(y) \cdot \nabla_x v_0(x, t). \tag{112}$$

Let  $\chi \in C^2(\mathbb{T}^d; \mathbb{R}^d)$  be the unique, mean-zero solution of the cell Eq. (39). If we choose  $v_1 = \chi \cdot \nabla_x v_0(x, t)$ , then it is clear that  $v_1$  solves (110).

Finally, by the Fredholm alternative on  $\mathcal{L}_0$ , a necessary condition for Eq. (111) to have a solution is that the RHS of (111) has mean zero with respect to the measure  $\rho$ , that is,

$$\frac{\partial v_0(x, t)}{\partial t} = \frac{1}{Z} \int_{\mathbb{T}^d} \mathcal{L}_1 v_1(x, y, t) \rho(y) \, dy + \frac{1}{Z} \int_{\mathbb{T}^d} \mathcal{L}_2 v_0(x, t) \rho(y) \, dy.$$

Substituting  $v_0$  and  $v_1$ , we obtain

$$\begin{aligned} \frac{\partial v_0(x, t)}{\partial t} &= \frac{1}{Z} \int_{\mathbb{T}^d} \nabla_y \cdot \left( \sqrt{|g|(y)} g^{-1}(y) \right) \cdot \nabla_x (\chi \cdot \nabla_x v_0(x, t)) \, dy \\ &\quad + \frac{2}{Z} \int_{\mathbb{T}^d} \sqrt{|g|(y)} g^{-1}(y) : \nabla_x \nabla_y (\chi \cdot \nabla_x v_0(x, t)) \, dy \\ &\quad + \frac{1}{Z} \int_{\mathbb{T}^d} \sqrt{|g|(y)} g^{-1}(y) : \nabla_x \nabla_x v_0(x, t) \, dy. \end{aligned}$$

Integrating the second term by parts with respect to  $y$  and simplifying, we obtain

$$\frac{\partial v_0(x, t)}{\partial t} = \left( \frac{1}{Z} \int_{\mathbb{T}^d} g^{-1}(y) (I + \nabla_y \chi(y)) \sqrt{|g|(y)} \, dy \right) : \nabla_x \nabla_x v_0(x, t),$$

where we have used the symmetry of  $g^{-1}$ . Thus, the homogenized diffusion equation for  $v_0$  is

$$\frac{\partial v_0(x, t)}{\partial t} = D : \nabla_x \nabla_x v_0(x, t), \tag{113}$$

where

$$D = \frac{1}{Z} \int_{\mathbb{T}^d} g^{-1}(y) (I + \nabla_y \chi(y)) \sqrt{|g|(y)} \, dy.$$

Multiplying (39) by  $\chi(y)\rho(y)$  and integrating by parts gives

$$\int_{\mathbb{T}^d} (I + \nabla_y \chi(y))^T g^{-1}(y) \nabla_y \chi(y) \sqrt{|g|(y)} \, dy = 0,$$

so that the effective diffusion matrix can be written in the following symmetric form

$$D = \frac{1}{Z} \int_{\mathbb{T}^d} (I + \nabla_y \chi(y))^\top g^{-1}(y) (I + \nabla_y \chi(y)) \sqrt{|g|(y)} \, dy.$$

From the limiting backward Kolmogorov equation (113), we can read off the limiting SDE  $dX^0(t) = \sqrt{2D} \, dB(t)$ . A rigorous proof of this result can be found in Duncan (2013).

### 12.2 Case II

Analogous to the previous case, we look for solutions  $v$  of the form

$$v^\varepsilon(x, \eta, t) = v_0(x, \eta, t) + \varepsilon v_1(x, \eta, t) + \dots,$$

for some smooth functions  $v_i : \mathbb{R}^d \times \mathbb{R}^K \times [0, T] \rightarrow \mathbb{R}^d$ . Substituting this ansatz in (72a) and identifying equal powers of  $\varepsilon$ , we obtain the following pair of equations

$$O\left(\frac{1}{\varepsilon}\right) : \mathcal{L}_0 v_0(x, \eta, t) = 0, \tag{114}$$

$$O(1) : \frac{\partial v(x, \eta, t)}{\partial t} = \mathcal{L}_0 v_1(x, \eta, t) + \mathcal{L}_1 v_0(x, \eta, t), \tag{115}$$

where  $(x, \eta, t) \in \mathbb{R}^d \times \mathbb{R}^K \times (0, T]$ .

The  $O(\frac{1}{\varepsilon})$  equation immediately implies that  $v_0$  is independent of the fast-scale fluctuations. The second equation then becomes

$$\mathcal{L}_0 v_1(x, \eta, t) = \frac{\partial v(x, \eta, t)}{\partial t} - \mathcal{L}_1 v_0(x, \eta, t).$$

Applying the Fredholm alternative, a necessary condition for the existence of a solution  $v_1$  is that the RHS is orthogonal to the invariant measure  $\rho_\eta$ , that is,

$$\frac{\partial v_0}{\partial t}(x, t) = \left[ \int_{\mathbb{R}^K} F(x, \eta) \rho_\eta(\eta) \right] \cdot \nabla v_0(x, t) + \left[ \int_{\mathbb{R}^K} \Sigma(x, \eta) \rho_\eta(\eta) \right] : \nabla \nabla v_0(x, t),$$

which is the backward equation for SDE (74).

### 12.3 Case III

We make the ansatz that

$$v^\varepsilon = v_0 + \varepsilon v_1 + \varepsilon^2 v_2 + \dots,$$

for some smooth functions  $v_i : \mathbb{R}^d \times \mathbb{T}^d \times \mathbb{R}^K \times [0, T] \rightarrow \mathbb{R}$ . Substituting  $v^\varepsilon$  in (82a) and identifying equal powers of  $\varepsilon$ , we obtain the following equations

$$O\left(\frac{1}{\varepsilon^2}\right) : \quad \mathcal{L}_0 v_0 = 0, \tag{116}$$

$$O\left(\frac{1}{\varepsilon}\right) : \quad \mathcal{L}_0 v_1 = -\mathcal{L}_\eta v_0 - \mathcal{L}_1 v_0, \tag{117}$$

$$O(1) : \quad \mathcal{L}_0 v_2 = -\left(\frac{\partial v_0}{\partial t} - \mathcal{L}_\eta v_1 - \mathcal{L}_1 v_1 - \mathcal{L}_2 v_0\right). \tag{118}$$

The first equation implies that  $v_0 \in \mathcal{N}[\mathcal{L}_0]$  so that  $v_0$  is a constant in  $y$ . The second equation thus becomes

$$\mathcal{L}_0 v_1(x, y, \eta, t) = (\mathcal{L}_\eta v_0(x, \eta, t) + F(y, \eta) \cdot \nabla_x v_0(x, \eta, t)).$$

By the Fredholm alternative applied to  $\mathcal{L}_0$ , we require that the RHS is centered with respect to  $\sqrt{|g|}$ , for each fixed  $x$  and  $\eta$  that is,

$$\int_{\mathbb{T}^d} (F(y, \eta) \cdot \nabla_x v_0(x, \eta, t) + \mathcal{L}_\eta v_0(x, \eta, t)) \sqrt{|g|(y, \eta)} \, dy = 0.$$

The first term in the above integral is clearly 0. Since  $\mathcal{L}_\eta v_0$  is independent of  $y$ , the centering condition becomes

$$Z(\eta) \mathcal{L}_\eta v_0(x, \eta, t) = 0.$$

Since  $Z > 1$ , it follows that  $v_0 \in \mathcal{N}[\mathcal{L}_\eta]$  is a sufficient condition for the centering condition to hold, which we therefore will assume. By ergodicity of the Ornstein–Uhlenbeck process  $\eta(t)$  over  $\mathbb{R}^K$ , it follows that  $v_0$  is also independent of  $\eta$  so that  $v_0$  is a function of  $x$  only. The second equation thus becomes

$$\mathcal{L}_0 v_1 = F(y, \eta) \cdot \nabla_x v_0.$$

Let  $\chi(\cdot, \eta)$  be the unique, mean-zero solution of the cell equation solution by the Fredholm alternative, since the centering condition holds. Choosing  $v_1 = \chi \cdot \nabla_x v_0$ , it is clear that  $v_1$  solves the  $O(\frac{1}{\varepsilon})$  equation.

We now consider the  $O(1)$  equation. By the Fredholm alternative, a necessary condition for the existence of a unique solution  $v_2$  is that the RHS is centered with respect to the invariant measure of  $\mathcal{L}_0$ , that is,

$$\frac{\partial v_0}{\partial t} = \int_{\mathbb{T}^d} (\mathcal{L}_\eta v_1 + \mathcal{L}_1 v_1 + \mathcal{L}_2 v_0) \rho_y \, dy,$$

which, substituting the definitions of the  $\mathcal{L}_i$ 's and  $v_j$ 's, can be written as follows:

$$\frac{\partial v_0}{\partial t} = \int_{\mathbb{T}^d} F \otimes \chi \rho_y \, dy : \nabla_x \nabla_x v_0 \tag{119a}$$

$$+ \int_{\mathbb{T}^d} g^{-1} \nabla_y \chi \rho_y + \nabla_y \chi g^{-1} \rho_y \, dy : \nabla_x \nabla_x v_0 \tag{119b}$$

$$+ \int_{\mathbb{T}^d} g^{-1} \rho_y \, dy : \nabla_x \nabla_x v_0 \tag{119c}$$

$$+ \int_{\mathbb{T}^d} \mathcal{L}_\eta \chi \rho_y \, dy \, \nabla_x v_0. \tag{119d}$$

First, we note that

$$\begin{aligned} \int_{\mathbb{T}^d} F(y, \eta) \otimes \chi(y, \eta) \sqrt{|g|(y, \eta)} \, dy &= - \int_{\mathbb{T}^d} \mathcal{L}_0 \chi(y, \eta) \otimes \chi(y, \eta) \sqrt{|g|(y, \eta)} \, dy \\ &= \int_{\mathbb{T}^d} \nabla_y \chi(y, \eta) g^{-1}(y, \eta) \nabla_y \chi(y, \eta)^\top \sqrt{|g|(y, \eta)} \, dy, \end{aligned}$$

so that we can write (119) as

$$\begin{aligned} \frac{\partial v_0}{\partial t} &= \int_{\mathbb{T}^d} (I + \nabla_y \chi) g^{-1} (I + \nabla_y \chi)^\top \rho_y \, dy : \nabla_x \nabla_x v_0 \\ &\quad + \int_{\mathbb{T}^d} \mathcal{L}_\eta \chi \rho_y \, dy \cdot \nabla_x v_0. \end{aligned}$$

Averaging with respect to the invariant measure  $\rho_\eta$  of  $\mathcal{L}_1$ , we derive the effective diffusion equation

$$\begin{aligned} \frac{\partial v_0}{\partial t} &= \int \int_{\mathbb{T}^d} (I + \nabla_y \chi) g^{-1} (I + \nabla_y \chi)^\top \rho_y \rho_\eta \, dy \, d\eta : \nabla_x \nabla_x v_0 \\ &\quad + \int \int_{\mathbb{T}^d} \mathcal{L}_\eta \chi \rho_y \rho_\eta \, dy \, d\eta \cdot \nabla_x v_0, \end{aligned}$$

or more compactly

$$\frac{\partial v_0}{\partial t} = D : \nabla_x \nabla_x v_0 + V \cdot \nabla_x v_0,$$

where  $D$  and  $V$  are given by (86) and (87), respectively. From the limiting backward Kolmogorov equation, we can read off the limiting SDE (85) for the process  $X^\varepsilon(t)$ .

### 12.4 Case IV

We look for solutions  $v$  of the form

$$v^\varepsilon = v_0 + \varepsilon v_1 + \varepsilon^2 v_2 + \dots$$

of (103a) for some smooth functions  $v_i : \mathbb{R}^d \times \mathbb{T}^d \times \mathbb{R}^K \times [0, T] \rightarrow \mathbb{R}$ . Substituting this ansatz in (103a) and equating equal powers of  $\varepsilon$ , we obtain the following three equations

$$O\left(\frac{1}{\varepsilon^2}\right) : \quad \mathcal{G} v_0 = 0, \tag{120}$$

$$O\left(\frac{1}{\varepsilon}\right) : \quad \mathcal{G} v_1 = -\mathcal{L}_1 v_0, \tag{121}$$

$$O(1) : \quad \mathcal{G}v_2 = - \left( \frac{\partial v_0}{\partial t} - \mathcal{L}_1 v_1 - \mathcal{L}_2 v_0 \right). \tag{122}$$

As the fast process is ergodic, the first equation implies that  $v_0$  is independent of  $y$  and  $\eta$ . The second equation thus becomes

$$\mathcal{G}v_1 = -F(y, \eta) \cdot \nabla_x v_0.$$

Since we are assuming Assumption (101), there exists a unique solution of the Poisson problem (100), by Proposition 8. By choosing  $v_1 = \chi \cdot \nabla_x v_0$ , we see that the second equation is satisfied.

By Proposition 8, a sufficient condition for the final equation to have a solution is that the RHS is orthogonal to the measure  $\rho(dy, d\eta)$ , (assuming that the RHS grows at most polynomially), that is,

$$\begin{aligned} \frac{\partial v_0}{\partial t}(y, \eta) &= \int F(y, \eta) \cdot \nabla_x v_1 \rho(dy, d\eta) + \int 2\Sigma(y, \eta) : \nabla_x \nabla_y v_1 \rho(dy, d\eta) \\ &\quad + \int \Sigma(y, \eta) : \nabla_x \nabla_x v_0 \rho(dy, d\eta), \end{aligned}$$

which we can rewrite as

$$\frac{\partial v_0}{\partial t} = D : \nabla_x \nabla_x v_0,$$

where the effective diffusion tensor  $D$  is given by

$$D = \int \left[ \frac{1}{\sqrt{|g|}} \nabla_y \cdot \left( \sqrt{|g|} g^{-1} \right) \otimes \chi + g^{-1} \nabla_y \chi^\top + \nabla_y \chi g^{-1} + g^{-1} \right] \rho(dy, d\eta)$$

Note that the first term on the RHS

$$\int \frac{1}{\sqrt{|g|}} \nabla_y \cdot \left( \sqrt{|g|} g^{-1} \right) \otimes \chi \rho(dy, d\eta) : \nabla_x \nabla_x v_0,$$

can be rewritten as  $\mathcal{H} : \nabla_x \nabla_x v_0$ , where

$$\mathcal{H} = \text{Sym} \left[ \int \frac{1}{\sqrt{|g|}} \nabla_y \cdot \left( \sqrt{|g|} g^{-1} \right) \otimes \chi \rho(dy, d\eta) \right],$$

where  $\text{Sym}[\cdot]$  denotes the symmetric part of the matrix. Let  $e \in \mathbb{R}^d$  be a unit vector and consider

$$\mathcal{H}^e := e \cdot \mathcal{H} e = \int \frac{1}{\sqrt{|g|}} \nabla_y \cdot \left( \sqrt{|g|} g^{-1} e \right) \chi^e \rho(dy, d\eta),$$

where  $\chi^e = \chi \cdot e$ . Noting that

$$-\mathcal{G}\chi^e = \frac{1}{\sqrt{|g|}} \nabla_y \cdot \left( \sqrt{|g|} g^{-1} e \right),$$

it follows that

$$\mathcal{H}^e = \int \chi^e (-\mathcal{G}\chi^e) \rho(dy, d\eta),$$

which, by (102), can be written as

$$\mathcal{H}^e = \int \nabla_y \chi^e \cdot g^{-1} \nabla_y \chi^e \rho(dy, d\eta) + \int \nabla_\eta \chi^e \cdot \Gamma \Pi \nabla_\eta \chi^e \rho(dy, d\eta),$$

so that

$$e \cdot De = \int (e + \nabla_y \chi^e) \cdot g^{-1} (e + \nabla_y \chi^e) \rho(dy, d\eta) + \int \nabla_\eta \chi^e \cdot \Gamma \Pi \nabla_\eta \chi^e \rho(dy, d\eta),$$

or in matrix notation

$$D = \int (I + \nabla_y \chi) g^{-1} (I + \nabla_y \chi)^T \rho(dy, d\eta) + \int \nabla_\eta \chi \Gamma \Pi \nabla_\eta \chi^T \rho(dy, d\eta),$$

as required. A rigorous proof of this result can be found in [Duncan \(2013\)](#).

## References

- Abdulle, A., Schwab, C.: Heterogeneous multiscale FEM for diffusion problems on rough surfaces. *Multiscale Model. Simul.* **3**(1), 195–220 (2005)
- Aizenbud, B.M., Gershon, N.D.: Diffusion of molecules on biological membranes of nonplanar form. II. Diffusion anisotropy. *Biophys. J.* **48**(4), 543–546 (1985)
- Almeida, P.F.F., Vaz, W.L.C.: Lateral diffusion in membranes. *Handb. Biol. Phys.* **1**, 305–357 (1995)
- Ashby, M.C., Maier, S.R., Nishimune, A., Henley, J.M.: Lateral diffusion drives constitutive exchange of AMPA receptors at dendritic spines and is regulated by spine morphology. *J. Neurosci.* **26**(26), 7046–7055 (2006)
- Axelrod, D., Koppel, D.E., Schlessinger, J., Elson, E., Webb, W.W.: Mobility measurement by analysis of fluorescence photobleaching recovery kinetics. *Biophys. J.* **16**(9), 1055–1069 (1976)
- Bensoussan, A., Lions, J.L., Papanicolaou, G.: *Asymptotic Analysis for Periodic Structures*, vol. 5. North Holland, NY (1978)
- Berg, H.C.: *Random Walks in Biology*. Princeton University Press, Princeton (1993)
- Borgdorff, A.J., Choquet, D., et al.: Regulation of AMPA receptor lateral movements. *Nature* **417**(6889), 649–653 (2002)
- Bourgeat, A., Jurak, M., Piatnitski, A.L.: Averaging a transport equation with small diffusion and oscillating velocity. *Math. Methods Appl. Sci.* **26**(2), 95–117 (2003)
- Brenner, S.C., Scott, L.R.: *The Mathematical Theory of Finite Element Methods*, vol. 15. Springer, Berlin (2008)
- Bressloff, P.C., Newby, J.M.: Stochastic models of intracellular transport. *Rev. Mod. Phys.* **85**(1), 135 (2013)
- Canham, P.B.: The minimum energy of bending as a possible explanation of the biconcave shape of the human red blood cell. *J. Theor. Biol.* **26**(1), 61–81 (1970)

- Coulibaly-Pasquier, K.A.: Brownian motion with respect to time-changing Riemannian metrics, applications to Ricci flow. In: *Annales de l'Institut Henri Poincaré, Probabilités et Statistiques*, vol. 47, pp. 515–538. Institut Henri Poincaré (2011)
- Crank, J.: *The Mathematics of Diffusion*. Oxford University Press, Oxford (1979)
- Deckelnick, K., Dziuk, G., Elliott, C.M.: Computation of geometric partial differential equations and mean curvature flow. *Acta Numer.* **14**, 139–232 (2005)
- Doi, M., Edwards, S.F.: *The Theory of Polymer Dynamics*, vol. 73. Oxford University Press, Oxford (1988)
- Duncan, A.B.: *Diffusion on Rapidly Varying Surfaces*. Ph.D. thesis, University of Warwick (September 2013)
- Dykhne, A.M.: Conductivity of a two-dimensional two-phase system. *Sov. J. Exp. Theor. Phys.* **32**, 63 (1971)
- Dziuk, G., Elliott, C.M.: Finite element methods for surface PDEs. *Acta Numer.* **22**, 289–396 (2013)
- Festa, R., d'Agliano, E.G.: Diffusion coefficient for a Brownian particle in a periodic field of force: I. Large friction limit. *Phys. A Stat. Mech. Appl.* **90**(2), 229–244 (1978)
- Friedman, A.: *Stochastic Differential Equations and Applications*, dover ed. edition. Dover Books on Mathematics. Dover Publications, New York (2006)
- Garnier, J.: Homogenization in a periodic and time-dependent potential. *SIAM J. Appl. Math.* **57**(1), 95–111 (1997)
- Gilbarg, D., Trudinger, N.S.: *Elliptic Partial Differential Equations of Second Order*, vol. 224. Springer, Berlin (2001)
- Gonzalez, O., Stuart, A.M.: *A First Course in Continuum Mechanics*. Cambridge University Press, Cambridge (2008)
- Gov, N.: Membrane undulations driven by force fluctuations of active proteins. *Phys. Rev. Lett.* **93**(26), 268104 (2004)
- Gov, N.S.: Diffusion in curved fluid membranes. *Phys. Rev. E* **73**(4), 041918 (2006)
- Granek, R.: From semi-flexible polymers to membranes: anomalous diffusion and reptation. *J. Phys. II* **7**(12), 1761–1788 (1997)
- Gustafsson, S., Halle, B.: Diffusion on a flexible surface. *J. Chem. Phys.* **106**, 1880 (1997)
- Halle, B., Gustafsson, S.: Diffusion in a fluctuating random geometry. *Phys. Rev. E* **55**(1), 680 (1997)
- Helfrich, W., et al.: Elastic properties of lipid bilayers: theory and possible experiments. *Z. Naturforsch. c* **28**(11), 693–703 (1973)
- Hsu, E.P.: *Stochastic Analysis on Manifolds*, vol. 38. American Mathematical Society, Providence, RI (2002)
- Jackson, J.L., Coriell, S.R.: Effective diffusion constant in a polyelectrolyte solution. *J. Chem. Phys.* **38**, 959 (1963)
- Karatzas, I.A., Shreve, S.E.: *Brownian Motion and Stochastic Calculus*, vol. 113. Springer, Berlin (1991)
- Keller, J.B.: Conductivity of a medium containing a dense array of perfectly conducting spheres or cylinders or nonconducting cylinders. *J. Appl. Phys.* **34**(4), 991–993 (1963)
- Khasminskii, R.Z., Yin, G.: Asymptotic series for singularly perturbed Kolmogorov–Fokker–Planck equations. *SIAM J. Appl. Math.* **56**(6), 1766–1793 (1996)
- Kim, S., Karrila, S.J.: *Microhydrodynamics: Principles and Selected Applications*. Dover Publications, NY (1991)
- King, M.R.: Apparent 2-D diffusivity in a ruffled cell membrane. *J. Theor. Biol.* **227**(3), 323–326 (2004)
- Kohler, W., Papanicolaou, G.C.: Bounds for the effective conductivity of random media. In: *Macroscopic Properties of Disordered Media*, pp. 111–130. Springer, Berlin (1982)
- Komorowski, T., Landim, C., Olla, S.: *Fluctuations in Markov Processes: Time Symmetry and Martingale Approximation*, vol. 345. Springer, Berlin (2012)
- Larsson, S., Thomée, V.: *Partial Differential Equations with Numerical Methods*, vol. 45. Springer, Berlin (2009)
- Leitenberger, S.M., Reister-Gottfried, E., Seifert, U.: Curvature coupling dependence of membrane protein diffusion coefficients. *Langmuir* **24**(4), 1254–1261 (2008)
- Lifson, S., Jackson, J.L.: On the self-diffusion of ions in a polyelectrolyte solution. *J. Chem. Phys.* **36**, 2410 (1962)
- Lin, L.C.L., Gov, N., Brown, F.L.H.: Nonequilibrium membrane fluctuations driven by active proteins. *J. Chem. Phys.* **124**(7), 074903–074903 (2006)
- Lin, L.C.L., Brown, F.L.H.: Dynamics of pinned membranes with application to protein diffusion on the surface of red blood cells. *Biophys. J.* **86**(2), 764–780 (2004)

- Lindblom, G., Orådd, G.: NMR studies of translational diffusion in lyotropic liquid crystals and lipid membranes. *Prog. Nucl. Magn. Reson. Spectrosc.* **26**, 483–515 (1994)
- Matheron, G.: *Éléments pour une théorie des milieux poreux*. Masson, Paris (1967)
- Mattingly, J.C., Stuart, A.M.: Geometric ergodicity of some hypo-elliptic diffusions for particle motions. *Markov Process. Relat. Fields* **8**(2), 199–214 (2002)
- Mattingly, J.C., Stuart, A.M., Higham, D.J.: Ergodicity for SDEs and approximations: locally Lipschitz vector fields and degenerate noise. *Stoch. Process. Appl.* **101**(2), 185–232 (2002)
- Mendelson, K.S.: A theorem on the effective conductivity of a two-dimensional heterogeneous medium. *J. Appl. Phys.* **46**(11), 4740–4741 (1975)
- Meyn, S.P., Tweedie, R.L.: *Markov Chains and Stochastic Stability*. Cambridge University Press, Cambridge (2009)
- Naji, A., Brown, F.L.H.: Diffusion on ruffled membrane surfaces. *J. Chem. Phys.* **126**, 235103 (2007)
- Papanicolaou, G.C.: Introduction to the asymptotic analysis of stochastic equations. *Mod. Model. Contin. Phenom.* (Ninth Summer Sem. Appl. Math., Rensselaer Polytech. Inst., Troy, NY, 1975) **16**, 109–147 (1977)
- Pardoux, É.: Homogenization of linear and semilinear second order parabolic pdes with periodic coefficients: a probabilistic approach. *J. Funct. Anal.* **167**(2), 498–520 (1999)
- Pavliotis, G.A., Stuart, A.M., Zygalakis, K.C.: Homogenization for inertial particles in a random flow. *Commun. Math. Sci.* **5**(3), 507–531 (2007)
- Pavliotis, G.A., Stuart, A.M.: *Multiscale Methods: Averaging and Homogenization*. Springer, Berlin (2008)
- Poo, M., Cone, R.A., et al.: Lateral diffusion of rhodopsin in the photoreceptor membrane. *Nature* **247**(441), 438 (1974)
- Reister, E., Seifert, U.: Lateral diffusion of a protein on a fluctuating membrane. *EPL (Europhys. Lett.)* **71**(5), 859 (2007)
- Reister-Gottfried, E., Leitenberger, S.M., Seifert, U.: Hybrid simulations of lateral diffusion in fluctuating membranes. *Phys. Rev. E* **75**(1), 011908 (2007)
- Reister-Gottfried, E., Leitenberger, S.M., Seifert, U.: Diffusing proteins on a fluctuating membrane: analytical theory and simulations. *Phys. Rev. E* **81**(3), 031903 (2010)
- Risken, H.: *The Fokker–Planck equation: methods of solution and applications*, vol. 18. Springer, Berlin (1996)
- Saxton, M.J., Jacobson, K.: Single-particle tracking: applications to membrane dynamics. *Annu. Rev. Biophys. Biomol. Struct.* **26**(1), 373–399 (1997)
- Sbalzarini, I.F., Hayer, A., Helenius, A., Koumoutsakos, P.: Simulations of (an) isotropic diffusion on curved biological surfaces. *Biophys. J.* **90**(3), 878 (2006)
- Seifert, U.: Configurations of fluid membranes and vesicles. *Adv. Phys.* **46**(1), 13–137 (1997)
- Stuart, A.M.: Inverse problems: a Bayesian perspective. *Acta Numer.* **19**(1), 451–559 (2010)
- Van Den Berg, M., Lewis, J.T.: Brownian motion on a hypersurface. *Bull. Lond. Math. Soc.* **17**(2), 144–150 (1985)
- Van Kampen, N.G.: *Stochastic Processes in Physics and Chemistry*. North Holland, Amsterdam (2007)
- Zhikov, V.V., Kozlov, S.M., Oleinik, O.A.: *Homogenization of Differential Operators and Integral Functionals*. Springer, Berlin (1994)